

## INFORMATION TO USERS

The most advanced technology has been used to photograph and reproduce this manuscript from the microfilm master. UMI films the original text directly from the copy submitted. Thus, some dissertation copies are in typewriter face, while others may be from a computer printer.

In the unlikely event that the author did not send UMI a complete manuscript and there are missing pages, these will be noted. Also, if unauthorized copyrighted material had to be removed, a note will indicate the deletion.

Oversize materials (e.g., maps, drawings, charts) are reproduced by sectioning the original, beginning at the upper left-hand corner and continuing from left to right in equal sections with small overlaps. Each oversize page is available as one exposure on a standard 35 mm slide or as a 17" × 23" black and white photographic print for an additional charge.

Photographs included in the original manuscript have been reproduced xerographically in this copy. 35 mm slides or 6" × 9" black and white photographic prints are available for any photographs or illustrations appearing in this copy for an additional charge. Contact UMI directly to order.



300 North Zeeb Road, Ann Arbor, MI 48106-1346 USA



**Order Number 8801719**

**A study of a meteor burst communication system**

**Hibshoosh, Eliphaz, Ph.D.**

**City University of New York, 1987**

**U·M·I**  
300 N. Zeeb Rd.  
Ann Arbor, MI 48106

---



**PLEASE NOTE:**

In all cases this material has been filmed in the best possible way from the available copy. Problems encountered with this document have been identified here with a check mark .

1. Glossy photographs or pages \_\_\_\_\_
2. Colored illustrations, paper or print \_\_\_\_\_
3. Photographs with dark background \_\_\_\_\_
4. Illustrations are poor copy \_\_\_\_\_
5. Pages with black marks, not original copy
6. Print shows through as there is text on both sides of page \_\_\_\_\_
7. Indistinct, broken or small print on several pages
8. Print exceeds margin requirements \_\_\_\_\_
9. Tightly bound copy with print lost in spine \_\_\_\_\_
10. Computer printout pages with indistinct print \_\_\_\_\_
11. Page(s) \_\_\_\_\_ lacking when material received, and not available from school or author.
12. Page(s) \_\_\_\_\_ seem to be missing in numbering only as text follows.
13. Two pages numbered \_\_\_\_\_. Text follows.
14. Curling and wrinkled pages \_\_\_\_\_
15. Dissertation contains pages with print at a slant, filmed as received \_\_\_\_\_
16. Other \_\_\_\_\_  
\_\_\_\_\_  
\_\_\_\_\_

**U·M·I**



**A STUDY OF A METEOR BURST COMMUNICATION SYSTEM**

**by**

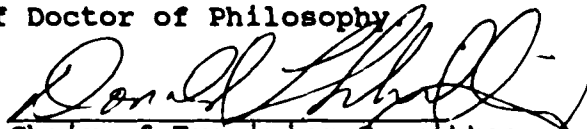
**Eliphaz Hibshoosh**

**A dissertation submitted to the Graduate Faculty  
in Engineering in partial fulfillment of the  
requirements for the degree of Doctor of Philosophy,  
The City University of New York.**

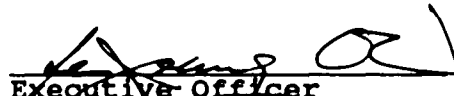
**1987**

This manuscript has been read and accepted for the Graduate Faculty in Engineering in satisfaction of the dissertation requirement for the degree of Doctor of Philosophy.

7/27/87  
Date

  
Chair of Examining Committee

July 27, 1987  
Date

  
Executive Officer

Prof. D. Ucci  
Prof. J. Barba  
Prof. T. Saadawi  
Supervisory Committee

The City University of New York

## ABSTRACT

### A STUDY OF A METEOR BURST COMMUNICATION SYSTEM

by

Eliphaz Hibshoosh

Adviser: Professor D.L. Schilling

This study discusses the use of the meteor burst channel in communication systems and has three main thrusts:

1) The development and enhancement of an accurate and reliable channel model based on recently available empirical data. Analysis of this model results in analytical expressions for communication parameters such as channel duration and throughput to be used as design and analysis tools.

2) The optimization of throughput for fixed transmission rate under the constraint of a given maximum bit error rate. This will demonstrate the room for improvement in existing systems using constant transmission rate.

3) The feasibility of efficiently communicating over the MBC using variable bit rate and employing a feedback protocol to monitor the channel. This approach will improve the throughput in comparison with constant transmission rate systems.

## ACKNOWLEDGEMENT

I wish to express my deep gratitude to professor Donald L. Schilling for the his interest, encouragement and valuable guidance during the progress of this research. The many technical discussions and his constructive suggestions are most appreciated.

I would like to thank all the members of my Doctoral Committee; Dean Paul Karmel, Professor Donald Ucci, Professor Joseph Barba and Professor Tarek Saadwi for the time and effort each has taken to read and constructively criticize this dissertation.

Special thanks to my parents and brothers and sisters for their constant support and encouragement. In addition, I would like to thank Ms. Victoria Godfrey and Mrs. Amy Hibshoosh for their excellent typing. Finally, thanks are due to the Lotus Corp. for its Manuscript software product.

## Table of Contents

1	STATEMENT OF THE PROBLEM .....	1
1.1	Introduction .....	1
1.2	Identification of the Problem .....	4
1.3	Significance of the Problem .....	6
1.4	Physical Properties of Meteor Trails .....	7
1.4.1	Meteoric Particles .....	8
1.4.2	Meteor Trails .....	13
1.4.3	Reflections Properties of Trails .....	17
1.4.4	Other Aspects .....	19
1.5	System Considerations .....	23
1.5.1	Point to Point Mode .....	23
1.5.2	Low Probability of Intercept (LPI) and Antijam (AJ) Consideration .....	25
1.5.3	System Performance .....	28
1.6	Past Systems .....	29
2	MATHEMATICAL MODEL AND CONCEPTUAL FRAMEWORK .....	32
2.1	Power Received and Related Parameters .....	32
2.1.1	Power Received from an Underdense Trail ...	32
2.1.2	Electron Line Density Statistics - Underdense Case .....	37
2.1.3	Decay Time Constant Statistics - Underdense Case .....	38
2.1.4	Joint PDF of $q$ and $B$ - Underdense Case ....	39
2.1.5	Power received from Overdense Trails .....	39
2.1.6	Electron Line Density Statistics - Overdense Case .....	42
2.2	Link Geometry .....	43
2.3	Trail Arrival .....	45
2.4	Power Spectral Density of the Received Noise ..	46
2.5	Modulation and Bit Error Rate .....	48
3	ANALYSIS AND RESULTS .....	50
3.1	Introduction and Approach .....	50
3.1.1	Protocol .....	54
3.2	Improvements .....	55
3.3	Sample System .....	57
3.4	Constant Bit Rate and Constrained BER System ..	59
3.4.1	Channel Duration .....	59
3.4.1.1	Burst Duration Statistics for Constant Bit Rate -- Underdense .....	60
3.4.1.2	Burst Duration Statistics for Constant Bit Rate -- Overdense .....	64
3.4.2	Bits per Given Burst .....	69
3.4.3	Throughput for Constant Bit Rate .....	76
3.4.3.1	Optimal Average Throughput for Constant Bit Rate System -- Underdense. ....	77
3.4.3.2	Optimal Average Throughput for Constant Bit Rate System -- Overdense. ....	83

3.4.3.3 Total Average Throughput for Constant Bit Rate System. ....	89
3.5 Variable Bit Rate and Constant BER System .....	92
3.5.1 Channel Duration .....	92
3.5.1.1 Transmission Duration for Variable Bit Rate -- Underdense .....	94
3.5.2 Throughput for Variable Bit Rate System - Underdense .....	96
3.5.3 Throughput for Variable Bit Rate System - Overdense .....	101
3.5.4 Comparison of Throughput for Constant and Variable Bit Rate Systems .....	103
4 DERIVATIONS .....	109
4.1 Link Geometry .....	109
4.2 Derivation of Average Burst Duration, Constant Bit Rate .....	110
4.3 Burst Duration Constant Bit Rate - Overdense ..	112
4.4 Optimal Average throughput for constant bit rate - Underdense .....	117
4.5 Transmission Duration & Throughput for Variable Bit Rate System .....	119
5 CONCLUSION AND IDENTIFICATION OF FUTURE WORK .....	122
6 TABLES .....	128
7 FIGURES .....	130
8 REFERENCES .....	148

## Table of Figures

1. Space Density Of Meteors- Seasonal Variation .....	130
2. Diurnal Variation In Meteor Activity .....	131
3. Correlation Patterns Near Mb Receiver .....	132
4. Geometry Of Meteor Burst-1 .....	133
5. Geometry Of Meteor Burst-2 .....	134
6. Geometry Of Meteor Burst-3 .....	135
7. Idealized Time Variations - Underdense And Overdense. ....	136
8. Power Received- Underdense .....	137
9. Pdf And Cdf Of Tb- Underdense (Case 1) .....	138
10. Pdf And Cdf Of Tb- Underdense (Case 2) .....	139
11. Burst Duration- Underdense .....	140
12. Burst Duration- Overdense .....	141
13. Bits Per Given Burst .....	142
14. Average Burst Duration - Underdense .....	143
15. Average Burst Duration - Overdense .....	144
16. Throughput Vs. Fixed Rate - Underdense .....	145
17. Throughput Vs. Wavelength- Fixed and Adaptive Rate .....	146
18. Throughput Vs. Fixed Rate - Overdense .....	147

**Table of Tables**

**Estimates of the Properties of Sporadic Meteors ..... 128**  
**Average Interval Between Bursts for the Comet System . 129**

## 1 STATEMENT OF THE PROBLEM

### 1.1 Introduction

There is currently an urgent need for alternate channels for communication. The large variety and quantity of users throughout the world have caused all of the existing channels to become extremely congested. A world wide search for such alternate channels is now being conducted for both present day and future communication systems through the use of different types of channels such as optical, laser, cable, satellite, etc. [14, 15, 17]

The particular application of Beyond-Line-of-Sight (BLOS) communications, which uses the High Frequency (HF) spectral band from 3 to 30 MHz, is very important to many current and potential users. However, HF is very sensitive to solar disturbances such as sunspot activity, solar storms and other galactic phenomena, as well as multipath returns from both ground and atmosphere, weather related attenuation, and other degrading factors [18,19]. Because of these factors a channel for communication is needed which has low congestion, is

robust and relatively indestructible, has very little outside interference and does not compete for bandwidth with existing communication systems. The research proposed herein represents such an alternative mode for communication.

Meteors are small aggregates of matter which upon entering the Earth's atmosphere burn up and form long columns or trails of ionized particles in the upper atmosphere at altitudes of 80 to 120 km. The ionized columns diffuse within seconds yet are able to support radio communication over a range of distance up to 2000 km by reflecting a radio signal and thus provide us with the so-called meteor burst channel (MBC). The frequency range used is from 30 to 100 MHz. The lower limit is dictated by the need to be above the HF range and avoid ionospherically reflected signals. The upper limit is set primarily by equipment sensitivity limitations since reflections at the higher frequencies are weaker than those at lower frequencies.

Excluding showers (annual Pleiades shower) the occurrence of a meteor burst appears in time to be random with a Poisson arrival and an average interval time on

the order of several seconds to minutes depending upon time of day, season, and global location, and communication system parameters.

Two types of trails are described in the literature: Underdense trails which are more frequent and have an electron line density below  $10^{14}$  e/m; and overdense trails which are less frequent and have electron line densities of more than  $10^{14}$  e/m. The power received from an underdense trail is approximated as an exponential time function whose initial amplitude is proportional to the square of the electron line density and the exponential decay time constant varies randomly from one trail to the next. The power received from an overdense trail is modeled by a complex time function whose shape for a given set of communication system parameters is determined by the value of the electron line density.

In the late fifties and early sixties, a considerable amount of research was conducted on the use of meteor burst communications for beyond line-of-sight (BLOS) transmission of digital data. In recent years, interest in meteor burst has been renewed because of several factors. The development of microprocessors (enabling inexpensive implementation of sophisticated system control procedures) and inexpensive solid-state memories

(for the buffering required to interface a burst transmission scheme to constant data sources and sinks) is partly responsible. In addition, the nuclear survivability of the meteor burst medium is superior to other BLOS media such as satellite and HF skywave, resulting in considerable interest in the military community.

## 1.2 Identification of the Problem

The research proposed herein represents such an alternative mode for BLOS communication. It relates a novel approach for BLOS communication. The approach is aimed at efficaciously using a previously under utilized and inefficiently used method of communication, namely, the Meteor Burst Channel (MBC) [1, 9]. This medium possesses all of the qualities mentioned above for a new communications channel. The channel operates in the relatively unused lower portion of the Very High Frequency (VHF) band ranging from 30 to 100 MHz. It avoids the degradations exhibited by HF on the low end and ionospheric phenomena at the high end. This region of the spectrum provides a sufficiently large bandwidth for efficient data communication. It is not easily

---

destroyed. It has a privacy feature inherent in its structure [1,9] and by virtue of its "newness" does not interfere with existing systems. For MBC, the antennas have a high elevation angle and rarely interfere with present use of the frequency band when such is present.

This study seeks to define systematically and analytically the limits of transmission of digital information over the meteor burst channel by using an improved model to develop the mathematical relationships among link geometry, communication circuitry parameters, physical meteor characteristics, modulation technique and a given communication protocol. Furthermore, the research will be aimed at the determination of optimal average throughput for both constant and variable transmission rates under the employment of an information feedback scheme for reliable channel monitoring.

These results will serve as a vital design and analysis tool for the communication system engineer using the MBC. Furthermore, they will demonstrate the viability and potential improvement over past and currently implemented systems. Finally, they will identify the necessary and challenging areas for future research.

### 1.3 Significance of the Problem

Meteor Burst communications has wide ranging effects for modern society. It offers simple and reliable communications and can operate in the simplex, half-duplex and full-duplex mode over distances of 200 to 1200 miles. [9,22]. Efficient use of this channel will result in increased data throughput for applications such as facsimile transmission (FAX), TELEX, transmission of computer data, radio amateur usage, voice burst transmission using phonemes (i.e., transmission in which the voice is digitally encoded using rates of 50 to 250 bits per second) and military communication systems. These types of communications and data transmission facilities involve transactions of banks, universities and medical centers, corporate business concerns such as online systems, and government agencies. In addition, recreational and pleasure or leisure activities could make use of this mode of communication.

If shown to be feasible and commercially cost effective business as well as home users could provide a potentially large market. The advent of the microprocessor will reduce the cost of such systems thus enabling inexpensive implementation of the control requirements to

be met [9,22,23]. This potential for low cost will open up the home and business market which has already invested millions of dollars in personal computers and modems. Furthermore, the number of these types of users is increasing daily.

Some of the government agencies interested in alternate communications means are the Department of Agriculture, the Department of Energy (DOE), the National Oceanic and Atmospheric Administration (NOAA), the Department of Defense (DOD), the National Aeronautics and Space Administration (NASA) and the Defense Communications Agency-(DCA) [9,22].

#### 1.4 Physical Properties of Meteor Trails

Nearly all of the present knowledge regarding the physical properties of meteors has been obtained from visual, optical, and radio observations of the trails formed by the meteoric particles as they enter the atmosphere of the earth. In this section the properties of the meteoric particles themselves and the trails which they form will be reviewed. The mathematical model and conceptual framework reflecting physical and radio

properties of the trail will be presented in chapter 2. The review of meteoric particles and the trails they form is from Sugar's [1] 1964 review paper.

#### 1.4.1 Meteoric Particles

For the purposes of this discussion the term "Meteors" will be used to apply to those particles entering the earth's atmosphere that are burned by frictional heating. This definition includes the very small particles, the micrometeorites, that slowly settle through the atmosphere without being destroyed. It also includes the large meteors which manifest themselves as fireballs or the even larger ones which reach the earth's surface as meteorites. The micrometeorites are not of concern because even though they are the most numerous of the various types, they enter the atmosphere too slowly to produce any significant ionization. The large meteoroids, although they produce substantial ionization, are of little concern here because their rate of occurrence is extremely low.

Some of the properties of meteoric particles are summarized in Table 1 [24], [25]. The particles of interest in meteor propagation are those with masses in

the range  $10^3$  to  $10^{-7}$  g and dimensions in the range 8 cm to 40 microns. Before being trapped by the gravitational field of the earth these particles move in orbits around the sun. Their composition is uncertain; however, they appear to be almost entirely of cometary origin. A substantial fraction of them are not single solid particles but fragile loosely-bound agglomerates, sometimes called "dustballs",

The meteors can be divided into two classes, the shower meteors and the sporadic meteors. The shower meteors are collections of particles all moving at the same velocity in fairly well-defined orbits or streams around the sun. Their orbits intersect the orbit of the earth at a specific time each year and at these times the well-known meteor showers are observed. In the cases where the particles are uniformly distributed around the orbit, the size of the shower varies little from year to year. If, on the other hand, there is a concentration of particles within the orbit, the extent of a shower can vary substantially in successive years. (The Leonid shower of 1833 is an example of an unusual display of meteor activity. During the peak of the shower as many as 20 meteor trails were often seen by a single observer in one second .) The shower meteors, while the most spectacular, account for only a small

fraction of all meteors. It is the nonshower or sporadic meteors that comprise nearly all of the meteors of interest in radio propagation. These meteors are those which do not have well-defined streams but rather seem to move in random orbits. Thus, whereas shower meteors appear to be coming from a specific point in the sky--the radiant point for the shower--sporadic meteors have radiants that appear to be randomly distributed over the sky.

The relation between sporadic and shower meteors is not clear at the present time. It is possible that the sporadic meteors represent the final stages in the decay of meteor streams. On the other hand there is some indication that the sporadic meteors are in fact distributed in a large number of relatively small groups and that the earth is immersed in about 11 such groups at a time. Further work is needed to resolve the origins of the sporadic meteors [1].

Shower meteors are most easily recognized in terms of their radiants, velocities, and time of occurrence, since these parameters are relatively fixed. The radiants and times of occurrence of sporadic meteors are random. Their radiant points are not, however, uniformly distributed in the sky but are for the most

part concentrated toward the ecliptic plane (the plane of the earth's orbit) and move in the same direction around the sun as the earth moves [26]. The orbits are not uniformly distributed along the earth's orbit but are concentrated so as to produce a maximum incidence of meteors at the earth in July and a minimum in February. This variation in the space density of meteors is shown in Fig. 1 which has been adapted from the data of Hawkins [26].

The rate of incidence of sporadic meteors at the earth is further modified by two factors. The first of these--resulting in a regular diurnal variation in meteor rate is illustrated in Fig. 2 . On the morning side of the earth, meteors are swept up by the forward motion of the earth in its motion around the sun. On the evening side the only meteors reaching the earth are those which overtake it. This results in a maximum occurrence rate around 6 a.m. and a minimum rate around 6 p.m. The ratio of maximum to minimum depends on the latitude of the observer. A further minor seasonal variation is introduced because of the tilt of the earth's axis relative to the ecliptic plane [27]. This variation, also dependent on the latitude of the observer, can change the expected hourly rates by factors as large as 1.4:1.

The mass distribution of sporadic meteors is such that there are approximately equal total masses of each size of particle. There are, for example, 10 times as many particles of mass  $10^{-4}$  g as there are particles of mass  $10^{-3}$  g. This approximate relation between particle mass and number is given in Table 1. The mass distribution of shower meteors is somewhat similar to that for the sporadic meteors with the important difference that there are more large particles relative to the number of smaller ones than for the sporadic meteors .

The velocities of meteors approaching the earth are in the range 11.3 to 72 km/sec. The lower limit is the escape velocity for a particle leaving the earth and is therefore the lowest velocity that a particle falling toward the earth can have. The upper limit is the sum of two components. a 30 km/sec component associated with the earth in its orbit around the sun, and a 42 km/sec component associated with the meteor itself. This latter velocity is the escape velocity for a particle leaving the solar system. Nearly all observations have indicated that meteor velocities fall in the above range and that the meteors are thus members of the solar system.

#### 1.4.2 Meteor Trails

1) Formation: As a meteoric particle enters the earth's atmosphere it collides with air molecules which then become trapped in its surface. The impact energy produces heat which evaporates atoms from the meteor and these move off with a velocity which is substantially equal to that of the meteor. Collisions between these high velocity atoms and the surrounding air result in the production of heat, light, and ionization, distributed in the form of a long, thin, paraboloid of revolution with the particle at the head of it. The electron line density in the trail is proportional to the mass of the particle. In the evaporation process each original impact frees many meteoric atoms and thus the total mass of air molecules striking the meteor is small compared to the meteoric mass itself. As a consequence the velocity of the meteor remains quite constant until the meteor is nearly completely evaporated. (Those meteors that appear to be dustballs rather than solid particles break up or "fragment" upon entering the atmosphere and proceed as a group of smaller particles. For this case

the above description appears to be correct if it is applied to the individual particles after fragmentation occurs.)

2) Heights: As a meteoric particle approaches the earth no appreciable ionization is formed until the particle enters the relatively dense air at heights below about 120 km. Above that height collisions of the particles with air molecules are not frequent enough to be of significance. As the particle traverses the region below about 120 km it vaporizes rapidly and most particles are completely evaporated before reaching 80 km. The relatively small thickness of the meteor region is a result of the rapid change in air density which occurs over the height range quoted. At 120 km the mean free path is 5.4 m and this decreases in an approximately logarithmic manner so that at 80 km it is only 3.8 mm.

The height distribution of trails varies somewhat with particle characteristics. The higher velocity particles produce trails at the higher heights with the mean trail height increasing to about 10 km as velocity increases from less than 15 km/sec to greater than 60 km/sec [1]. The particles of higher mass produce maximum trail ionization at lower heights. Over the

mass range of  $10^3$  to  $10^{-7}$  g the height variation is around 44 km. There is also a height variation with the zenith angle of the trail orientation, with the larger angles corresponding to greater heights. A variation of about 13 km is associated with nearly the whole range of zenith angles.

3) Lengths: The lengths of meteor trails are primarily dependent on particle mass and zenith angle. Typical lengths range up to 50 km with the most probable trail length for sporadic meteors being 15 km. (Several definitions of "length" can be used and the one chosen here uses as end points the points with a threshold value chosen.)

4) Initial Radius: Until recently it has been assumed that, at the time of their formation, trails had an initial radius of the order of the mean free path or at most about 14 times this radius. However, photographic and radio measurements have suggested that the initial radius is significantly larger than indicated above and that this increase is probably associated with the dustball and fragmentation hypothesis.

The trail radii indicated by these measurements are in the range 0 to 1.2 m (with a mean value of 0.65 m) for the photographic work, and 0.55 to 4.35 m for the radio work. The 0.55 m was for a height of 81 km where the mean free path is only  $5 \times 10^{-8}$  m. The results at 121 km are more nearly consistent with Manning's hypothesis since the initial radius observed is 4.35 m and the mean free path is 5 m.

5) Dissipation: Once the trail is formed it expands by diffusion [21] at a relatively low rate, producing a radial distribution of material that is approximately Gaussian. The quantity  $(4Dt + r^2)$  may be taken as the approximate radius of the trail after a time  $t$  where  $D$  is the diffusion coefficient and  $r$  is the initial radius of the trail.  $D$  varies from  $1 \text{ m}^2/\text{sec}$  at an 85 km height to  $140 \text{ m}^2/\text{sec}$  at 115 km. Thus after one second a trail will have a radius in the range 2 to 20 m.

The practical lifetime of a trail is of course dependent on the means for detecting it. Most trails detected by radio means are those resulting from small particles and these last only a fraction of a second. The larger particles produce more densely ionized trails and trails with durations of the order of a

minute are observed several times per day. Trails with durations of the order of an hour or more are extremely rare.

The dissipation of trails is further complicated by the presence of winds in the meteor region. At the time of formation trails are quite straight but they are rapidly deformed by these winds which have typical velocities of the order of 25 m/sec and vertical gradients with mean relative maxima of about 100 m/sec/km. A wind shear of this magnitude can rotate part of a trail through an angle of  $5^{\circ}$  in one second.

#### 1.4.3 Reflections Properties of Trails

The distribution of energy reflected by a meteor trail is a function of many variables. The ionization density distribution across and along the trail, the orientation of the trail, the radio wavelength, the polarization of the incident wave relative to the trail, motion of the trail either as part of the process of formation or due to ionospheric winds, and the straightness of the trail are all significant. In discussing the reflection properties it is convenient to divide the trails into two classes underdense trails

and overdense trails and to examine the properties of each class independently. Underdense trails are those wherein the electron density is low enough so that the incident wave passes through the trail and the trail can be considered as an array of independent scatterers. Overdense trails are those wherein the electron density is high enough to prevent complete penetration of the incident wave and to cause reflection of waves in the same sense that the ordinary ionospheric reflections occurs. A rough sorting of trails into these two categories can be done on the basis of trail lifetime or duration. At long wavelengths the underdense trails have durations of less than about one second while the overdense trails have longer durations. At long wavelengths the effective duration of a trail is large compared to the time it takes the trail to form, and the trail may be considered to have a cylindrical shape.

The solutions to be considered here are useful approximations to the physical problems. They will apply quite well to some of the trails observed and rather poorly to others. A complete analysis of the reflections from even a relatively simple trail would be far too complex to be of any practical use or interest.

---

#### 1.4.4 Other Aspects

In this section some additional practical aspects will be discussed from a qualitative viewpoint. The discussion is directed toward the long wavelength cases since relatively few short wavelength observations have been made and analyzed.

1) Long Wavelength Reflections during Trail Formation: The transient state associated with trail formation is of interest since it accounts for some of the observed characteristics of trail reflections. As a trail is being formed, but before the meteor reaches the first Fresnel zone, a weak reflection is obtained from the incomplete trail. This comes primarily from the part of the trail corresponding to the shortest transmission path at the instant; and when, as is usually the case, this is the head of the trail, the reflected signals are shifted in frequency because of the motion of the effective reflecting point. As the meteor approaches the first Fresnel zone for the trail this frequency shift approaches zero, and thus the received frequency decreases with time. The observed frequency will of course depend on trail orientation,

meteor velocity and observing wavelength. A maximum shift of the order of 5 kHz is possible for 50 MHz forward-scatter observations over a 1000 km path.

2) Trail Drift and Distortion: The effects of ionospheric winds are appreciable for trails which last for the order of a second or more. A Doppler shift of the received frequency will be associated with the average wind velocity of the trail. For a velocity of 25 m/sec this "body Doppler" can be as large as 18 Hz for backscatter observations at 50 MHz and will be somewhat less for forward-scatter observations.

The trail distortion resulting from wind shears can lead to the formation of several local first Fresnel zones for the trail since a distorted trail can have several points where the transmission path length has a local minimum. These local minima, or "glints" as they have been called [41], are strong scatters and the received signal is a composite of their contributions. Since they are moving at different velocities the signals from each have different Doppler shifts and the resultant composite signal fades in an irregular manner [24]. (At 50 MHz the fading rate observed for forward scatter are of the order of 1-10 Hz.) In addition to producing the fading observed for long-enduring trails

the wind shears can rotate a trail sufficiently to produce reflections when the initial orientation has not been suitable. Thus these trails lose their aspect sensitivity as time goes on, and if their life is of the order of 10 seconds they will scatter in all directions.

3) Polarization Effects: Thus far the only indication that the polarization of the incident wave can be of significance was the inclusion of the  $\sin^2(\alpha)$  term in each of the transmission equations for the forward-scatter cases. This term accounts for the foreshortening of the electric vector of the incident wave which occurs when it is viewed from the receiver. In addition to this, a kind of electron resonance can occur which increases the reflection coefficient for the trail. This is associated with the restoring force that the electrons experience as the incident electric field displaces them from their equilibrium positions in a direction normal to the trail. This resonance can occur only for underdense trails and only then for trail diameters much less than the wavelength. This resonance at most doubles the reflection coefficient and thus can increase the received power by a factor of 4.

4) Diversity Effects: Underdense trails act as small coherent sources, and therefore CW signals scattered by them exhibit good space and frequency correlation. Correspondingly, very little pulse broadening is observed when pulse signals are used. The limited available data, suggest that for a forward-scatter path about 1000 km in length, operating near 50 MHz the correlation coefficient observed for single underdense trails will fall to 0.5 for antenna spacings of the order of 150 km along the path, for antenna spacings of the order of 30 km across the path, and for frequency separations greater than 5 MHz. Three micro-sec pulses show no appreciable broadening under these conditions.

Overdense trails, in contrast to the underdense trails, tend to act like relatively large sources and therefore exhibit much poorer space and frequency correlation properties. Again, as in the underdense case, specific data on these properties are not available. Present results suggest that the correlation observed for single overdense trails will fall to 0.5 for antenna spacings of the order of 50 [41]. Measurements using short pulses over a 1000-km path indicate that the received composite signal can have a total time spread as large as 10 micro-sec [44].

## 1.5 System Considerations

There are three potential modes of operation for a meteor burst system: point-to-point, netted, and broadcast. While a meteor burst system could be operated in any or all of these modes, all known meteor burst systems that have currently been implemented have been designed for point-to-point applications. In this section, we discuss some of the possibilities for configuring meteor burst systems in point to point mode. This general review is from Oetting's [9] 1980 paper.

### 1.5.1 Point to Point Mode

The point-to-point mode is, of course, straightforwardly implemented. The only requisite for effective system control is the ability of the transmitting terminal to discern, as accurately as possible, the beginning and end of a useful burst. If transmission begins too late or ends too soon, valuable burst time will be wasted. If the transmission extends past the useful portion of the burst, a high error rate will result.

In all point-to-point systems, we assume that a feedback path is available. In the half-duplex case, the forward and return links share the same frequency, while in the full-duplex case, they use two different frequencies. For achieving data transmission between point A and point B, perhaps the simplest strategy is to assign a different frequency to each transmitter and to continuously transmit a probe signal from the master station (say, point A). When point B detects the probe, he transmits a preamble followed by his information. Point A uses the preamble to synchronize his receiver and is subsequently able to receive data. It is usually required that A acknowledge the reception of the message or block of data.

Several variations of this basic point-to-point approach have been developed. Early meteor burst systems used a signal amplitude threshold to determine if the probe signal were being received. The JANET system [1]-[13] improved upon this procedure by substituting a signal-to-noise ratio measurement for the fixed threshold test, thereby reducing the false alarm rate. After extensive testing of the JANET B system, the SHAPE Technical Centre concluded that, even with the SNR approach, a suitable compromise between efficient use of the channel and low error rate was not

achievable. Thus, they developed their own approach using ARQ with one teletype character per seven-bit block. This approach is referred to as the COMET system [5] and [9].

The possibilities for netted meteor burst systems have not been well explored to date. The only known system capable of netted operation is the Western Union hardware currently being installed for the Department of Agriculture [28]. This system will consist of 511 remote sites that communicate with two master stations. Although the Department of Agriculture application involves one-way transmission of data from the remote to the master stations, the system can be configured to provide two-way data transmission. A network could then be achieved by having a master station operate in a store-and-forward mode.

#### 1.5.2 Low Probability of Intercept (LPI) and Antijam (AJ) Consideration

One of the primary attractions of meteor burst communications is its inherent privacy resulting from the restricted footprint of reflections from meteor trails. This property has received considerable

attention in the meteor burst literature and has prompted a large number of industry proposals to provide LPI meteor burst systems for numerous Department of Defense (DoD) and non-DoD agencies.

Signals propagating between a specific transmitter and receiver can normally be detected by an eavesdropping receiver only if the latter is located in an elliptically bounded "footprint" in the vicinity of the primary receiver. By reciprocity, interfering signals from a remote transmitter will propagate to a meteor burst receiver only if the interfering transmitter is within the footprint of the desired transmitter. Measurements indicate that the major and minor axes of the footprint are on the order of 2000 and 25 mi, respectively. Clearly, the footprint is not a well-defined boundary within which the signal is always received and beyond which it is never received. Instead, the situation is better depicted by Fig. 3 which shows theoretical and experimental results for the correlation between the signals detected by two different receivers as a function of the distance between them. When the unintended receiver is moved in a direction perpendicular to the transmission path, the

correlation falls off more rapidly than when the unintended receiver is moved along the propagation path. [9]

While the theoretical along-the-path correlation falls off at an alarmingly slow rate, the experimental results illustrate two key points: the theoretical performance is difficult to achieve in practice, and the correlation decreases at higher operating frequencies. In addition, it has been shown [29] that fading reflections are responsible for a significant part of the correlation at large separations (trails that have been distorted by winds exhibit broader reradiation patterns than newly formed trails). By communicating only during the nonfading portion of each burst, the size of a footprint can be kept to a minimum.

LPI is best achieved by operating in a burst mode with a low duty cycle. While interception by a beyond-the-horizon transmitter is then governed by the probabilities shown in Fig. 3, a meteor burst system is vulnerable to line-of-sight interception unless spread spectrum techniques are employed.

As for AJ considerations, line-of-sight jamming can be easily accomplished in view of the losses incurred by the desired signal in the course of being reflected

from a meteor trail. In the case of beyond-the-horizon jamming, the jammer can disrupt only a small fraction of the traffic if he relies on reflections from meteor trails to propagate his jamming signals. A much better strategy is to use extremely high power (perhaps in a pulsed model) and rely on ionosscatter propagation. This approach can be defeated by operating at the higher meteor burst frequencies, since ionosscatter falls off much faster with increasing frequency than does meteor trails reflections. Finally, a jammer can attempt to spoof the system by transmitting a simulated probe signal, but spoofing can be defeated by judicious system design.

### 1.5.3 System Performance

The performance parameters of greatest interest in commercial applications are the average throughput (in bit per second), the average waiting time (to transmit a message of specific length), and the probability of error. These parameters will be influenced to varying degrees by the environmental variables: background noise level, external interference, geographic location, season, and time of day. The system designer, on

the other hand, can exert control over system performance by manipulating his design variables - transmitted power, RF frequency, instantaneous data rate, modulation technique and antenna gain.

The throughput of a meteor burst system depends on factors such as transmitted power, operating frequency, communications range, received noise and instantaneous data rate. The increase in throughput that can ultimately be attained is limited by intersymbol interference due to multipath effects, practical bit synchronization problems, and, of course, the available transmitter power and antenna gains.

In addition to the factors under the control of the system designer, the throughput also depends on such environmental variables as time of day and season of the year. These variations typically involve a factor of five diurnally and three seasonally.

## 1.6 Past Systems

A landmark meteor trail communication system was operational in the 1950s--the Canadian JANET system (after Janus, the Roman god who looks both ways at once).'

---

It was used for teletype communications between Toronto and Port Arthur, a distance of approximately 1000 km [1],[4]. A double sideband AM duplex channel was used to transmit and receive cosine-squared shaped pulses in pulse position modulation (ppm) at a rate of 650 bits per second (bps). Punched paper tape, magnetic tape, and a toriodal magnetic matrix storage core were used as storage media to compress messages in time for transmission and to store and expand the messages at the receiving station. Despite its relative antiquity, the JANET system embodied many of the features of today's systems: stored digital data which is transmitted/received in bursts after carrier detection, duplex operation at VHF frequencies around 50 MHz, and low effective duty cycles (about 0.1 for the JANET system). Other links, such as a one way Bozeman, MONTANA-Stanford, California meteor burst link were also operational during the 1950s, but the JANET system represents the first mature, complete, practical hardware implementation of a meteor burst system.

Subsequent experimental tests were conducted during the 1960s and 1970s. Notable among these efforts is the experimental work summarized by Sugar [4] and the implementation of the COMET (COMMunication by METeor Trails) system which has operated between the Netherlands

---

and Southern France. COMET made use of frequency diversity and Automatic Repeat for reQuest (ARQ) which allowed for signal repetition in the event of no radio path. The COMET system used a 2000 baud signaling rate and FSX with a 6 KHz deviation. The storage devices were similar to those of the JANET system. COMET demonstrated the practicality of meteor burst communications under a variety of conditions. Typical results indicated successful transmission of a 50 baud (average) message, 150 characters long with a delay of about a minute. Worst case delays of 3 or 4 minutes were typical [5]. Studies of COMET-type systems have continued into the 1980s [5][9].

## 2 MATHEMATICAL MODEL AND CONCEPTUAL FRAMEWORK

In this chapter the basic equations that model the meteor burst channel are presented. In addition, basic assumptions, constraints and empirical factors are stated.

### 2.1 Power Received and Related Parameters

The power received from the trail model used here is from the classic paper by Eshelman and Manning [6] and Hines and Forsyth [16].

#### 2.1.1 Power Received from an Underdense Trail

Meteor trails with fewer than  $10^{14}$  electrons per meter of length are referred to as underdense. Eshelman has shown that a simple Fresnel description of the process is normally sufficient. The scattering then is specular for the majority of received signals, that is the incident and scattered rays make equal

angles  $\delta$  with the axis of the trail and the received signal comes, in effect, from the principal Fresnel zone alone. See Fig. 4

The principal Fresnel zone is centered on a point P in the trail at a distance  $R_T$  and  $R_R$  from the transmitter T and receiver R respectively such that  $R_T + R_R$  is a minimum for the trail in question. The received power rises rapidly in the fraction of a second taken by the meteor to traverse the principal zone and reaches a peak volume at time  $t=0$ .

Although the meteor trail is formed as a narrow column, a few centimeters in diameter, it immediately begins to expand by diffusion. As the diameter increases, the scattered signal suffers increasingly from a destructive interference of the fields scattered by individual electrons. In ideal circumstances, neglecting Fresnel ripples and initial diameter, the received power decays exponentially in time, see fig. 7. The above is summarized in the next equation.

$$P(t) = \frac{P_T G_T G_R r_e^2 \sin^2(\alpha) \lambda^3 \exp\left(-\frac{8\pi^2 r_0^2}{\lambda^2 \sec^2 \phi}\right)}{16\pi^2 R_T R_R (R_T + R_R) (1 - \cos^2 \beta \sin^2 \phi)} q^2 \exp\left(-\frac{32\pi^2 D}{\lambda^2 \sec^2 \phi} \cdot t\right)$$

where,

(2.1.1-1)

$P_T$  Transmitter power.

$G_T, G_R$  Transmitter and receiver antenna gains, respectively.

$r_e$  Classical radius of an electron ( $2.82 \cdot 10^{-15}$  m).

$\alpha$  Angle between the electron field vector  $E$  and  $R_R$ .

$q$  Electron line density of the trail.

$\lambda$  Carrier wavelength.

$r_0$  Initial radius of the trail (.65 m.).

$\phi$  Angle of incidence/reflection of the transmitted plane wave.

$R_T$  Distance from transmitter to trail.

$R_R$  Distance from receiver to trail.

$D$  Diffusion coefficient of the atmosphere.

$\beta$  Angle between the trail and the propagation plane formed by  $R_T$  and  $R_R$ .

Figures 4, 5, and 6 depict the geometrical parameters.

A minimal set of assumptions is applied in the literature [7,11,21] for analysis:

- 1.) The trail occurs at midpoint between receiver and transmitter i.e.  $R_T = R_R$
- 2.) The burst occurs at an altitude of 100 km.
- 3.) The trail is travelling at a plane perpendicular to the plane formed by  $R_T$  and  $R_R$  i.e.  $\beta = \pi/2$ . In addition, we set  $\alpha = \pi/2$ .

Under these assumptions and after substituting for the physical constants we rearrange the above equation to arrive at the power received equation for the underdense case.

$$P(t) = C_U q^2 e^{-t/\bar{B}} \quad (2.1.1-2)$$

where,

$$C_U = 2.5179581 \cdot 10^{-32} \cdot \frac{P_T G_T G_R \lambda^3 \exp\left(-\frac{33.359}{\lambda^2 \sec^2 \phi}\right)}{R_T^3}$$

$$\bar{B} = 3.166 \cdot 10^{-3} \cdot \frac{\lambda^2 \sec^2 \phi}{D}$$

It should be emphasized that:

- 1.)  $P(0)$ , the maximum power from the underdense trail is proportional to  $q^2$ ; for a specific trail  $q$  is fixed. (The random character of  $q$  is discussed later).
- 2.)  $C_U$ , the constant of proportionality, incorporates the effects of link geometry, transmitter power,

antenna gains and carrier wavelength. For a given communication system  $C_U$  is constant since link distance, transmitter power, antenna gains and carrier frequency are set.

3.) The decay time constant  $B$  given above is found to be randomly varying from trail to trail. The expression in the classic model corresponding to a decay time constant is taken as the average decay time constant in accordance with observations. To date, however, researchers have assumed all underdense trails to share the same decay time constant to facilitate their analysis. It is in this added complexity to the model that our treatment deviates from published analysis and enhances its accuracy.

4.) The decay time constant  $B$  and the electron line density  $q$  are functionally independent [1] [7] and hence statistically independent.

5.) For a given communication system (i.e.  $C_U$  fixed) knowledge of the electron line density  $q$ , and decay time constant  $B$ , completely specify the underdense trail behavior in time.

### 2.1.2 Electron Line Density Statistics

#### - Underdense Case

Based on recent empirical data [33] the pdf for  $q$  is:

$$f_q(q) = Qq^{-p} \quad q_{\min} \leq q \leq q_u = 10^{14} \text{ e/m} \quad (2.1.2-2)$$

where,

$$Q = (p-1)q_{\min}^{p-1} \cdot \frac{1}{1 - \left(\frac{q_{\min}}{q_u}\right)^{p-1}}$$

$$p = 1.6$$

$q_{\min}$  = Minimum  $q$  as explained below.

$q_{\min}$  is the minimum electron line density  $q$  a trail must possess to be 'seen' by the communication system i.e.  $C_U q_{\min}^2$  is the minimum power level  $P_{\min}$  detected by the communication system. In the context of constant transmission rate systems ( as discussed later )  $P_{\min}$  is the power level that corresponds to the maximum allowed bit error rate. See fig. 8

### 2.1.3 Decay Time Constant Statistics

#### - Underdense Case

We start by stating that the expected value of the decay time constant  $B$  is well approximated by:

$$E(B) = \bar{B} = 3.16610^{-3} \cdot \frac{\lambda^2 \text{sec}^2 \phi}{D} \quad \text{sec} \quad (2.1.3-1)$$

as defined in section 2.1.1

The random decay time constant  $B$  is assumed to be exponential or Rayleigh. Both assumptions have been shown to be consistent with recent experimental observation [33]. In general the Rayleigh distribution will be used since for very small  $B$  ( extremely fast decay ) the probability is very near zero. This is appealing from a physical viewpoint and consistent with observation. It should also be noted that even if such exceedingly fast decaying trails occur they are of no utility for communication.

Exponential:

$$f_B(b) = \frac{1}{\bar{B}} e^{-b/\bar{B}} \quad (2.1.3-2)$$

where  $\bar{B}$  is defined above.

Rayleigh:

$$f_B(b) = \frac{b}{\alpha^2} e^{-b^2/2\alpha^2} \quad (2.1.3-3)$$

where,

$$\alpha = \sqrt{\frac{2}{\pi}} B$$

#### 2.1.4 Joint PDF of q and B - Underdense Case

Since the electron line density and the decay time constant are statistically independent the joint pdf is given by their product i.e.  $f_{q,B}(q,b) = f_q(q) \cdot f_B(b)$  (2.1.4-1)

where the individual densities are given in the previous sections.

#### 2.1.5 Power received from Overdense Trails

Trails with more  $10^{14}$  electrons per meter are often termed "overdense." When treating them, it is no longer satisfactory to think of the incident wave as penetrating the trail without serious modification. Instead, coupling between individual electrons plays a

prominent part, and the whole of the scattering process is conceived more simply in terms of reflections from a cylindrical surface.

The surface in question surrounds the axis of the trail at a radius  $r$ , where the electron volume density has the critical value normally associated with reflection of the incident wave (cf. reflection from the ionosphere). The volume density within the trail exceeds the critical value, and cannot support propagation in the usual sense at the pertinent frequency. As the electrons diffuse outwards,  $r$  increases from an initially small value, passes through a maximum, and falls to zero as the volume density at the axis of the trail decreases below the critical value. In the very latest stages the scattering reverts to the underdense type, but only after some time, and so only when the underdense scattering is extremely small.

The scattering process is again specular, the angles of incidence and reflection being equal. The received power variation is given by:

$$P(t) = C'_0 \sqrt{\frac{r_0^2 + 4Dt}{\sec^2 \phi}} \ln \left( \frac{r_0 \lambda^2 \sec^2 \phi}{\pi^2 (r_0^2 + 4Dt)} \cdot q \right) \quad (2.1.5-1)$$

where,

$$C'_0 = \frac{P_T G_T G_R \sin^2(\alpha) \lambda^2}{32 \pi^2 R_T R_R (R_T + R_R) (1 - \cos^2 \beta \sin^2 \phi)}$$

and all other parameters are as defined for the underdense burst.

Using the same assumptions as for underdense case ( $\alpha = \beta = \pi/2$  and  $R_T = R_R$ ) and some algebra we rewrite the above as:

$$P(t) = C_0 \sqrt{(k+t) \cdot \ln \left( \frac{a \cdot q}{k+t} \right)} \quad t \leq aq - k \quad (2.1.5-2)$$

where,

$$C_0 = 3.16628610^{-3} \sqrt{D} \frac{P_T G_T G_R \lambda^2}{R_T^3}$$

$$k = .105625/D$$

$$a = 7.14314310^{-17} \cdot \frac{\lambda^2 \sec^2 \phi}{D}$$

As in the underdense case we have rearranged the classic equation for ease of handling. Note that  $C_0$

contains the transmitted power, antenna gains, diffusion coefficient, carrier frequency and the effects of link distance. Fig. 7

In addition, from eq. (2.1.1-2) we relate  $C_U$  and  $C_O$  by

$$C_o = 1.257481610^{29} \frac{\sqrt{D}}{\lambda} \cdot e^{\left(\frac{30 \cdot 369}{1^2 \cdot \text{mc}^2 \cdot \epsilon}\right)} \cdot C_U \quad (2.1.5-3)$$

#### 2.1.6 Electron Line Density Statistics

##### - Overdense Case

Based on recent empirical data [33] the pdf for  $q$  is:

$$f_q(q) = Qq^{-p} \quad q_{\text{min}0} \leq q \leq q_{\text{uo}} = 10^{16} \text{ e/m} \quad (2.1.6-2)$$

where,

$$Q = (p-1)q_{\text{mino}}^{p-1} \cdot \frac{1}{1 - \left(\frac{q_{\text{mino}}}{q_{\infty}}\right)^{p-1}}$$

$$p = 1.5$$

$q_{\text{mino}}$  = Minimum  $q$  as explained below.

$q_{\text{mino}}$  is the minimum electron line density  $q$  an overdense trail must possess to be 'seen' by the communication system. Note that  $q_{\text{mino}} > q_{\text{Lo}}$  the (physically) lowest possible electron line density for an overdense trail.  $q_{\text{Lo}} = 10^{14}$  e/m. We define another constant which we refer to later as:

$$Q' = 1 / [1 - (q_{\text{mino}}/q_{\text{Lo}})^{p-1}].$$

## 2.2 Link Geometry

In this section we present the relationship between link distance,  $L$ , and station to trail distance,  $R_T$  ( $=R_R$ ) and angle of incidence/reflection  $\phi$ . See Fig. 6

The station to trail distance is given by

$$R_T = R_R = \sqrt{(h + L^2/8R_0)^2 + L^2/4} \quad (2.2-1)$$

And the incidence/reflection angle  $\phi$  is found thru

$$\sec^2(\phi) = 1 + \frac{L^2}{\left(2h + \frac{L^2}{4R_e}\right)^2} \quad (2.2-2)$$

where,

- h trail altitude (100 km).
- L great circle distance between stations.
- $R_T$  distance from transmitter to trail.
- $R_R$  distance from receiver to trail.
- $R_e$  radius of the earth, 6400 km.

The derivation of the above is done in section. 4.1

Since it is often convenient to express L and the resulting  $R_R$  in thousands of kilometers for ease of computation we then have:

$$R_T = R_R = \sqrt{(.1 + (.01953)L^2)^2 + L^2/4} \quad (2.2-3)$$

$$\sec^2(\phi) = 1 + \frac{L^2}{(0.2 + (.039)L^2)^2} \quad (2.2-4)$$

s.t. for  $L=1000$  km. we use  $L=1$  to quickly yield  $R_T=R_R = 514$  km. and  $\sec^2 \phi = 18.5$

### 2.3 Trail Arrival

In this section we are concerned with quantifying the trail arrival process in terms of communication system parameters. Since the arrival is Poisson we need to estimate the average time between bursts or equivalently the number of bursts per second. Oetting, [9] summarized the results of the COMET system showing an average time between bursts of 4 to 20 seconds.

It is often necessary to estimate the number of arrivals of bursts per second with an electron line density of  $q$  between some  $q_1$  and  $q_2$ . We let  $A'(q)$  be the number of trails/s with an electron line density between  $q$  and  $q+dq$  e/m. Using Weitzen [10] we write

$$A'(q) = \frac{19.1667 \cdot \phi \sin \phi \cdot (R_R \xi)^2}{q^2} \quad q_{\min} \leq q \leq q_{\max} = 10^{17} \quad (2.3-1)$$

where  $\xi$  is the idealized beamwidth of the antenna and all other parameters have been previously defined. The number of trails/s with  $q$  in a given range  $[q_1, q_2]$ ,  $A$ , is found by integrating the above density over  $q$  yielding the following

$$A = \frac{19.1667 \cdot \phi \sin \phi (R_R \zeta)^2}{q_1} \left[ 1 - \frac{q_1}{q_2} \right] \quad (2.3-2)$$

$$A = \frac{19.1667 \cdot \phi \sin \phi (R_R \zeta)^2}{q_1} \left[ 1 - \frac{q_1}{q_2} \right] \quad (2.3-2)$$

note that for overdense trails ( $q_1 > 10^{14}$ ) we scale the constant 19.1667 in the above Eq. to be 3.

In addition, care must be exercised in setting  $q_{\min}$  since this is an empirical relationship. For example, for a 1000 km link with antenna angle of  $46^\circ$   $q_{\min}$  must be above  $10^{13}$  e/m for the formula above to yield reasonable rates.

Finally, we mention again the dependence of the number of bursts/s, A, on other factors such as global location, time of day, and season. These factors should appropriately scale any value of A used for analysis.

#### 2.4 Power Spectral Density of the Received Noise

For signal frequencies appropriate to the MBC the dominant noise sources are galactic and man-made in origin. Consequently, the received noise power spectral,

density,  $N_0$ , is a function of the galactic noise picked up by the receiver antenna and the receiver thermal noise.

$N_0$  is modeled as follows:

$$N_0 = kT_0 \left[ \frac{104}{L_R} \left( \frac{\lambda}{15} \right)^{2.3} + F \right] \quad (2.4-1)$$

where,

$k$  = Boltzmann constant,  $1.3805 \cdot 10^{-23} J/K$

$T_0$  =  $290^\circ K$

$L_R$  = power loss between the antenna and receiver

$F$  = receiver noise figure

$\lambda$  = wavelength in meters

We choose typical values for  $L_R$  and  $F$  as 1.3 and 2.5, respectively to yield the following model for  $N_0$

$$N_0 = 4 \cdot 10^{-21} \left[ 80 \left( \frac{\lambda}{15} \right)^{2.3} + 2.5 \right] \text{ W/Hz} \quad (2.4-2)$$

## 2.5 Modulation and Bit Error Rate

The bit error rate, BER, denoted here as  $P_b$ , is in general related to the bit energy  $E_b$  and power spectral density of the received noise  $N_0$  as

$$P_b(t) = g\left(\frac{E_b(t)}{N_0}\right) \quad (2.5-1)$$

where  $g(\cdot)$  is determined by the modulation technique.

Since  $E_b(t) = P(t)/R(t)$  where  $R(t)$  the bit transmission rate may be time varying or fixed we have from Eq. (2.5-1)

$$P_b(t) = g\left(\frac{P(t)}{N_0 R(t)}\right) \quad (2.5-2)$$

or alternatively, we can solve for the power

$$P(t) = N_0 \cdot R(t) \cdot g^{-1}(P_b(t)) \quad (2.5-3)$$

where

$g^{-1}(\cdot)$  is the inverse of  $g(\cdot)$ .

For BPSK we have:

$$P_b(t) = \frac{1}{2} \operatorname{erfc} \left( \sqrt{\frac{P(t)}{N_0 R(t)}} \right) \quad (2.5-4)$$

and 
$$P(t) = N_0 \cdot R(t) [\operatorname{erfc}^{-1}(2 \cdot P_b(t))]^2 \quad (2.5-5)$$

For BFSK we have:

$$P_b(t) = \frac{1}{2} \exp \left( -\frac{1}{2} \cdot \frac{P(t)}{N_0 R(t)} \right) \quad (2.5-6)$$

and 
$$P(t) = N_0 \cdot R(t) \cdot \ln \left( \frac{1}{2 P_b(t)} \right) \quad (2.5-7)$$

### 3 ANALYSIS AND RESULTS

This chapter presents and explain our approach and reasoning to the use and analysis of the MB channel. The significant analytical expression to be used as design and analysis tools are given.

#### 3.1 Introduction and Approach

As stated earlier, our aim in the analysis is to arrive at a set of analytical relationships for important communication parameters such as burst duration and throughput using as accurate a model as possible. These relationships will serve as analysis and design tools where the effects of system parameters and constraints (power, geometry, BER) on throughput can be assessed. Our goal is to estimate the optimal average throughput for a given communication system.

Two types of communication systems are considered:

1) A system with a constant transmission rate and a time varying bit error rate which is constrained not to exceed some maximum allowable value.

2) A system employing a variable transmission rate which mimics the time varying power in order to maintain a practically constant bit energy and BER for all transmitted bits.

For the constant bit rate system, since the power is time varying, the probability of bit error will be time varying in a fashion dictated by the relevant modulation function. Specifically, for the underdense burst we have an exponentially decaying power in time and consequently the BER is monotonically increasing. Whether underdense or overdense we see the need then to impose a ceiling on the BER. For such systems, where the probability of bit error is time varying, we specify a maximum allowable BER,  $P_{bmax}$ , such that all transmitted bits shall have a BER less than or equal to  $P_{bmax}$ . This constraint on the probability of bit error for constant transmission rate systems implies the existence of a minimum power level  $P_{min}$  such that all transmitted bits have a received power greater than or equal to  $P_{min}$ . Such is obvious when remembering that the modulation function relating power to BER is an increasing function for decreasing argument.'

In short,  $P_b(t) = P_{bmax}$  when  $P(t) = P_{min}$ . The time for which the power received from the meteor burst exceeds a prescribed threshold ( $P_{min}$ ) is the burst duration  $t_B$  (also duty cycle [1]).

Clearly the duration of time for which the received power  $P$  is greater than  $P_{min}$  varies from one meteor burst to the next. For a constant bit rate system the burst duration is crucial in determining the number of bits transmitted during a given burst and ultimately in estimating throughput. We shall therefore analyse its relationship to system parameters, derive its statistics and compare it with current dogma.

As we increase our set constant bit rate the corresponding  $P_{min}$  has to be increased resulting in shortening the effective duration of transmission. This clear tradeoff between transmission rate and duration of transmission,  $t_B$ , suggests an optimal choice for transmission rate (or equivalently an optimal  $t_B$ ) so as to maximize the throughput. The link between the number of bits transmitted per burst and throughput is done through the average arrival rate statistics and trail shape statistics (variation in  $q$  and/or  $B$ ). The

judicious choice of transmission rate for the given system provides us, therefore, with the optimal throughput.

The second type of communication system considered here is a variable transmission rate system. Under such a system the bit rate mimics the time behavior of the received power (or equivalently stated the bit duration varies in a reciprocal manner to the received power variation) so as to maintain a constant bit energy. The direct outcome of such approach is a constant probability of bit error. More importantly, we note that we are not restricted by the need to operate above a prescribed threshold of received power; for as the power diminishes we simply compensate by increasing the bit duration. This adaptive approach implies, theoretically at least, for the underdense burst an infinitely long time of transmission. This of course, is offset by the practical limitation on bit duration and the need to maintain a fairly constant BER. The assumption here is that the hardware is fast enough to vary the transmission rate (bit duration) from one bit to the next. Since the power in most cases diminishes during the duration of the bit, for long bit duration we deviate from the requirement to maintain a constant bit energy and constant BER. It is, therefore necessary to take this fact into account in

determining the duration of transmission. This criterion of allowing only a small drop in the assumed constant bit energy imposes a restriction on the maximum bit duration which in turn limits the duration of transmission. As in the previous case we estimate the throughput by averaging over the ensemble of trails and incorporating the effects of trail arrival statistics. Finally, we express the correct packet probability in terms of the modulation function, packet length and communication system parameters.

### 3.1.1 Protocol

Both stations have receiving and transmitting capabilities. The station which acts as transmitter of data listens continuously for a continuous tone which is being sent from the receiver. Upon detection of this tone both the presence and the strength of the channel is known to the transmitter which immediately commences transmission. The situation is completely symmetrical with respect to the receiver. Clearly, the beginning of the burst, i.e. availability of the channel, is known to the transmitter within a negligible

propagation delay (less than 3.5 msec for a 1000 km link). The continuous tone used for monitoring the channel is at a different frequency than the data for ease of gating and synchronizing. For constant bit rate systems the essential feature of this scheme is the ability of the transmitter to discern the beginning of the burst. For variable bit rate systems the strength of the channel as gauged by the transmitter in addition to the burst's start are important for adaptive bit rate determination.

The above description is the rudimentary layer upon which additions and refinements could be made.

### 3.2 Improvements

The advantages of the analysis herein stem basically from considering a more complex MBC model than found in the literature. Most researchers [9, 21] while acknowledging the significant contribution to communication of the rare yet robust overdense burst have tended to concentrate on the underdense burst phenomenon because its simpler exponential form is more mathematically tractable. Able [11], however, does analyze the

overdense trail by a piecewise linear (first order) approximation resulting in conservative channel duration estimation. We choose a second order approximation to improve the fit of the overdense transcendental power time function. This yields better results for channel duration for the overdense case. For the exponential case, researchers to date have assumed a fixed decay time constant. Hampton [21] in his analysis of an MB broadcast system used a constant decay rate which was the conditional expected time constant given a fixed burst duration. This approach, however, implies that the decay time constant is dependent upon an average of a function of the electron line density whereas it is known that the time constant is independent of the electron line density. To enhance the accuracy of our model we chose to adhere to empirical results and assume the decay time constant to be a random quantity independent of the electron line density.

Some researchers [34] have further simplified the MBC model by assuming a fixed electron line density for all exponential bursts. This is contrary to experimental observation. Here, as in the case of the exponential decay time constant, we incorporate this random parameter into our model.

In analyzing throughput we compare two systems: constant bit rate system and variable bit rate system and derive the average throughput for both. For constant bit rate we derive the expression for the optimal average throughput. This optimal average throughput is achieved by finding the "best" bit rate to be used for the communication system so as to maximize throughput for the underdense burst. This is not to be confused with the optimal bit rate for a given burst that maximizes the number of transmitted bits for the burst under consideration.

In summary we note that the bedrock of a communication system using the MBC is its model. To enhance the analysis we used a model with as few simplifications as possible while maintaining mathematical tractability.

### 3.3 Sample System

For quantitative appreciation of the results we need to assume some values for a communication system. The set of these assumed parameters values will comprise what will heretofore be referred to as our sample system. This

sample communication system represents practical or average values. Chapter 2 contains the definition of the parameters.

$L$  = 1000 km link distance. From section 2.2 we have for the next two parameters:

$\sec(\phi)$  = 18.5 and

$R_T = R_R$  = 514 km.

$P_T$  = 1000 w

$G_T$  = 10 dB.

$G_R$  = 10 dB. And for antenna beamwidth we use

$\zeta$  =  $45.84^\circ$  (.8 rad)

$\lambda$  = 6 m. (50 MHz)

$D$  = 8 m<sup>2</sup>/s

$P_{bmax}$  =  $10^{-5}$  Max. BER for constant bit rate system.

Using BPSK modulation we get:

$g^{-1}(P_{bmax}) = 9$

$$N_0 = 4 \cdot 10^{-21} \left[ 80 \left( \frac{\lambda}{15} \right)^{2.3} + 2.5 \right] \text{ W/Hz}$$

See discussion above Eq. (2.4-2).

$N_0$  =  $4.89 \cdot 10^{-20}$  at 50 MHz.

For comparison the BER for variable rate system,  $P_b$ ,  
is set equal to  $P_{bmax}$   
 $R_{minV}$  = 1000 b/s (minimum variable rate allowed)

### 3.4 Constant Bit Rate and Constrained BER System

#### 3.4.1 Channel Duration

Channel duration or burst duration,  $t_B$  is the time for which the power received from the burst exceeds a given minimum value  $P_{min}$ . It is also the duration of data transmissions for a given burst where all bits possess a probability of error less than some maximum allowable BER,  $P_{bmax}$ .  $P_{min}$  is determined thru the modulation function by the following parameters: Transmission rate (non-time-varying), power spectral density of the received noise, and the maximum allowable bit error rate. The burst duration  $t_B$  is determined by  $P_{min}$  and  $C_u$  which incorporates system parameters such as transmitter power, link geometry effects, carrier wavelength etc.

**3.4.1.1 Burst Duration Statistics for**  
**Constant Bit Rate -- Underdense**

The channel duration,  $t_B$ , - burst duration - is the time of transmission for a given burst i.e. the usable portion of the burst, assuming a constant transmission rate,  $R$ , some given maximum allowed BER, and power spectral density,  $N_0$ , see Fig. 11.

For such conditions for the underdense burst we have:

$$t_B = B \cdot \ln \left( \frac{q}{q_{\min}} \right)^2 \quad (3.4.1.1-1)$$

where

$$q_{\min} = \sqrt{\frac{P_{\min}}{C_U}}$$

$$P_{\min} = N_0 \cdot R \cdot g^{-1}(P_{b\max})$$

and

$$C_U = 2.517958110^{-32} \cdot \frac{P_T G_T G_R \lambda^3 \exp\left(-\frac{33.359}{\lambda^2 \sec^2 \phi}\right)}{R_T^3}$$

or equivalently

$$t_B = B \cdot \ln \left( \frac{C_U}{N_0 \cdot R \cdot g^{-1}(P_{b\max})} \cdot q^2 \right) \quad (3.4.1.1-2)$$

We now average over the ensemble of underdense bursts (averaging over  $q$  and  $b$ ) to yield the average burst duration:

The Average Burst Duration-- Underdense:

$$\bar{t}_B = \frac{2B}{p-1} \cdot \frac{1}{1-x} \cdot [1-x(1-\ln x)] \quad (3.4.1.1-3)$$

where

$$x = \left( \frac{q_{\min}}{q_U} \right)^{p-1} = \left[ \frac{N_0 \cdot R \cdot g^{-1}(P_{b\max})}{C_U q_U^2} \right]^{\frac{p-1}{2}}$$

and

$$B = 3.16610^{-3} \cdot \frac{\lambda^2 \sec^2 \phi}{D} \quad q_U = 10^{14} \quad p = 1.6$$

$$R_N = \frac{R}{R_{\max}} = \left( \frac{q_{\min}}{q_U} \right)^2$$

$$R_{\max} = \frac{C_U q_U^2}{N_0 g^{-1}(P_{b\max})}$$

For a given communication system  $C_U$ ,  $R$ ,  $N_0$ ,  $P_{b\max}$ ,  $B$  and  $g(\cdot)$  are specified.  $R_N$  is the normalized (with respect to the highest possible rate for an underdense burst) bit rate.

Fig. 14 plots the above the above for our sample system (Sec. 3.3) as a function of  $R_N$ . ( $R_N=1--R=86.5$  kb/s)

The variance of  $t_B$  is given by:

$$\sigma_{t_B}^2 = \frac{4}{(p-1)^2} \cdot \frac{1}{(1-x)^2} [c_1 \sigma_B^2 + c_2 B^2] \quad (3.4.1.1-4)$$

where

$$c_1 = 2 - x(3 + y^2) + x^2(1+y^2)$$

$$c_2 = 1 - x(2+\ln^2(x)) + x^2$$

$$y = 1 - \ln(x)$$

$x$  from previous equation

and

$$\sigma_{t_B} = \frac{2}{(p-1)(1-x)} \sqrt{kc_1 + c_2} \cdot B \quad (3.4.1.1-5)$$

For B Rayleigh  $k = \frac{4}{\pi} - 1$ . For B exponential  $k = 1$

The  $n^{\text{th}}$  moment of  $t_B$  is given by:

$$\bar{t}_B^n = \frac{2^n \bar{B}^n}{(p-1)^n} \cdot \frac{n!}{1-x} \cdot \left\{ 1 - x \sum_{i=0}^n (-1)^i \frac{\ln^i(x)}{i!} \right\}$$

The PDF and CDF of  $t_B$  are:

$$f_{t_B}(t_1) = p' Q' \int_{b_{\min}}^{\infty} \frac{1}{b} \exp\left(\frac{-p' t_1}{b}\right) f_B(b) db \quad (3.4.1.1-6)$$

$$F_{t_B}(t_1) = Q' \left\{ 1 - x F_B(b_{\min}) - \int_{b_{\min}}^{\infty} \exp\left(\frac{-p' t_1}{b}\right) f_B(b) db \right\} \quad (3.4.1.1-7)$$

where

$x$  and  $p$  are from above eq. (3.4.1.1-3)

$$p' = (p - 1)/2$$

$$b_{\min} = t_1 / [ (1/p') \ln(1/x) ]$$

$$Q' = 1/(1-x)$$

For the case of  $x \ll 1$  i.e.  $P_{\min} \ll C_U q_U^2$ , essentially ignoring  $P_{b_{\max}}$  (considering all physical trails) we have for the solution of the above integrals ( $b_{\min} = 0$ ):

**B assumed exponential:**

$$f_{t_B}(t_1) = 2 \frac{p'}{B} \cdot K_0(z) \quad (3.4.1.1-8)$$

and

$$F_{t_1}(t_1) = 1 - z K_1(z) \quad t_1 \geq 0 \quad (3.4.1.1-9)$$

$$\text{where } z = \sqrt{4 \frac{P}{B} \cdot t_1}$$

where,  $K_0$  and  $K_1$  are the modified Hankel functions of order 0 and 1 respectively.

**B assumed Rayleigh:**

$$\begin{aligned} F_{t_1}(t_1) &= 1 - 2 \int_0^{\infty} b \exp(-b^2 - t_1/b) db & (3.4.1.1-10) \\ &= 1 - 2f_1(t_1) \end{aligned}$$

where  $f_1(t_1)$  is a tabulated function [35]. See Fig. 9.

The above results are presented in greater detail in ref. [12]

### 3.4.1.2 Burst Duration Statistics for

#### Constant Bit Rate -- Overdense

An exact solution to the roots of the power

received equation - overdense - is not known. The difference between these time instances yields the duration of the channel. We can approximate the power function in a piecewise linear fashion (comprised of two straight lines) or alternatively use a second order approximation. The second order approximation used here improves the accuracy of the results.

The results are stated without the lengthy derivation. For derivation see section 4.3

$$t_B = .95 a q \sqrt{1 - \frac{q_T}{q}} \quad q_{\min} \leq q \leq q_{\max} = 10^{16} e/m \quad (3.4.1.2-1)$$

where

$a$  and  $C_0$  are from Eq (2.1.5-2)

$$q_T = (e/a) (P_{\min}/C_0)^2 = q_{\max} R_{NO}^2$$

$R_{NO} = R/R_{\max}$ , normalized bit rate.

$$R_{\max} = C_0 [a q_{\max}/e]^{.5} / N_0 g^{-1}(P_{b\max})$$

maximum possible bit rate for any

overdense

burst.

$$q_{\min} = \max(q_T, q_{LO}) \quad q_{LO} = 10^{14} \quad q_{\max} = 10^{16} e/m.$$

$e$  is the natural logarithm base.

Note that  $q_{LO}$  is the minimum (physical) electron line density that can support an overdense burst.  $q_T$  is specified by our choice of system parameters and bit rate and may not correspond to a real level of overdense electron line density. See discussion following Eq. (3.4.1.2-3). See Fig. 12. but note that in the figure  $q_T < q_{LO}$ .

We can also relate  $q_T$  to  $q_{min}$  recalling the definition of  $P_{min} = C_U q_{min}^2$  ;

$$q_T = \frac{e}{a} \left( \frac{C_U}{C_0} \right)^2 q_{min}^4 \quad (3.4.1.2-2)$$

where the parameters  $C_U$ ,  $C_0$ ,  $a$  and  $q_{min}$  are defined in Eqs. (2.1.1-2) and (2.1.5-2) and (3.4.1-1) respectively.

#### Average Burst Duration - Overdense:

The average burst duration for the overdense case is found by averaging over the ensemble of bursts, yielding

$$i_s = 1.9aQ\sqrt{q_T} \left\{ \sqrt{\frac{q_{uo}}{q_T} - 1} - \sqrt{\frac{q_{mino}}{q_T} - 1} + \cos^{-1} \left( \sqrt{\frac{q_T}{q_{mino}}} \right) - \cos^{-1} \left( \sqrt{\frac{q_T}{q_{uo}}} \right) \right\}$$

(3.4.1.2-3)

where,

$$q_{mino} = \max\{q_T, q_{LO}\}$$

$$q_T = q_{uo} \cdot R_{NO}^2$$

$$R_{NO} = \frac{R}{R_{maxo}}$$

$$R_{maxo} = \frac{C_o \sqrt{a \cdot q_{uo}}}{\sqrt{e \cdot N_o \cdot g^{-1}(P_{bmax})}}$$

$R_{NO}$  is the normalized bit rate with respect to the maximum rate possible for any overdense burst,  $R_{maxo}$ . Note that the above can be expressed as two functions one for  $q_T < q_{LO}$  (or equivalently  $R_{NO} < .1$ ) where  $q_{mino} = q_{LO}$  and the other for  $q_T > q_{LO}$  (or equivalently  $R_{NO} > .1$ ) where  $q_{mino} = q_T$ . In addition, the value of  $Q$  varies with the domain as well since  $Q$  is a function of  $q_{mino}$  - see Eq. (2.1.6-2). For the case where  $R_{NO} > .1$  ( $q_T > q_{LO}$ ) we have

$$Q = .5(q_{uo}) \cdot .5 R_{NO} / (1 - R_{NO})$$

For the case where  $R_{NO} < .1$  ( $q_T < q_{LO}$ ) we have

$$Q = .5(q_{LO}) \cdot .5 / .9$$

Fig. 15 plots the above for our sample system (Sec. 3.3) as a function of  $R_{NO}$ . ( $R_{NO}=0.1$ -- $R=256$  kb/s)  
 For many practical systems we generally have  
 $q_T \ll q_{LO} \ll q_{UO}$  i.e.  $q_{mino} = q_{LO}$ ,  $Q = (q_{LO})^{1/2}/2$   
 resulting in:

$$t_B = .95a \cdot \sqrt{q_{UO}q_{LO}} \quad (3.4.1.2-4)$$

and for  $q_T < .01 q_{UO}$  we have for the burst duration variance:

$$\sigma_{t_B}^2 = .95 \frac{a^2}{3} \sqrt{q_{LO}q_{UO}^3} = .95 \frac{a^2}{3} 10^{31} \quad (3.4.1.2-5)$$

For our sample system defined in Sec. 3.3 the standard deviation of  $t_B = 11$  sec.

Burst Duration pdf and cdf - Overdense:

CDF of  $t_B$ :

$$F_{t_B}(t_1) = \left\{ \begin{array}{l} 0 \quad t_1 \leq t_{1min} \\ Q \cdot \left[ 1 - \left( \frac{2}{q_T} \frac{q_{mino}}{1 + \sqrt{1 + (t_1/\tau)^2}} \right)^{p-1} \right] \quad t_{1min} \leq t_1 \leq t_{1max} \end{array} \right\} \quad (3.4.1.2-6)$$

where

$p=1.5$  and

$$t_{1 \min} = .95 a q_{\min} \sqrt{1 - \frac{q_T}{q_{\min}}} \quad q_{\min} = \max\{q_T, q_{LO}\}$$

$$t_{1 \max} = .95 a q_{UO} \sqrt{1 - \frac{q_T}{q_{UO}}}$$

$$\tau = .95 \frac{a q_T}{2} = .95 \frac{e}{2} \left( \frac{P_{\min}}{C_0} \right)^2$$

PDF of  $t_B$ :

$$f_{t_B}(t_1) = (p-1) \frac{Q}{\tau^2} \left( \frac{2q_{\min}}{q_T} \right)^{p-1} \left[ (1+z)^{-p} \cdot \frac{t_1}{z} \right] \quad t_{1 \min} \leq t_1 \leq t_{1 \max}$$

(3.4.1.2-7)

where

$$z = \sqrt{1 + \left( \frac{t_1}{\tau} \right)^2}$$

and all other parameters are defined by previous equations.

### 3.4.2 Bits per Given Burst

Bits per given burst under constant bit rate and

constrained BER is the number of bits transmitted for the burst whose  $q$  and/or  $B$  are known. Since the bit rate,  $R$ , is assumed constant the number of bits,  $N_B$ , is simply the product of  $R$  times the burst duration  $t_B$  as defined in previous sections. Clearly, the level of power  $P_{\min}$  which reciprocally affects  $t_B$  is dictated by the modulation function and in general increases with increasing bit rate  $R$ . As a result we see the trade-off between the bit rate,  $R$ , and transmission duration,  $t_B$ , such that increasing one decreases the other. This suggests the existence of an optimal bit rate,  $R^*_B$ , (or equivalently, optimal transmission duration) that maximizes the number of bits transmitted during the given burst. Clearly, using any bit rate other than the optimal  $R^*_B$  will result in under-utilization of the burst. Alternatively stated, given a bit rate one should transmit only for as long as the optimal burst duration dictates. The optimal bit rate for the given burst is then used to calculate the maximum number of bits,  $N_B^*$ , that can be transmitted during this burst. A ratio is then obtained for the same burst between the number of bits transmitted using variable bit rate (BER constant =  $P_{b\max}$ ) and the  $N_B^*$  using constant bit rate. This ratio has been shown by Abel [11] to be around 2.5. Using the "best" (highest

q) burst for overdense and underdense trails bounds can be found for the maximum possible  $N_B^*$  (constant rate system) and maximum transmitted bits using variable rate.

Two points however, must be kept in focus:

1) Since  $R^*$  varies from trail to trail and a priori knowledge of the trail behavior is impossible to obtain, the optimal (constant) bit rate for the system, i.e. for all possible bursts, is still unknown. Paranthetically, we note that attempting to find the burst's shape from knowledge of its beginning is both wasteful of valuable transmission time and unreliable since many bursts deviate from ideal behavior. As will be shown, the important parameter for throughput determination is not  $N_B$  -- the number of bits for a given burst -- but rather the number of bits per burst averaged over the ensemble of all bursts since the latter is directly proportional to the average throughput.

2) While it is true that more bits can be transmitted using variable bit rate during the burst rather than employing constant bit rate, the situation is somewhat analogous to an apples/oranges comparison. For the underdense burst and constant bit rate all bits except the last one will possess a BER smaller than  $P_{bmax}$  --

the worst BER, whereas for variable bit rate all bits will possess the same BER =  $P_{bmax}$ . Consequently, the probability of having an error-free packet of data is higher for constant bit rate than for variable bit rate.

We present the analysis for the given underdense burst by first considering constant bit rate with constrained BER and then considering variable bit rate system with constant BER.

#### Constant Bit rate system

Given an underdense burst -  $q$  and  $B$  are assumed known.  $P_{bmax}$  is specified for the system and  $R$  is the constant bit rate. Let  $N_B$  be the number of bits transmitted on this burst. All bits have  $BER < P_{bmax}$ . All bits have power  $P > P_{min}$ . From the discussion on burst duration and the above definition of  $N_B$  we have:

$$N_B = R \cdot t_B \quad (3.4.2-1)$$

Using eq. (3.4.1.1-2) for  $t_B$  we rewrite the above as

$$N_B = R \cdot B \cdot \ln(R_0/R) \quad (3.4.2-2)$$

$$\text{where } R_0 = C_u q^2 / N_0 g^{-1}(P_{bmax})$$

Note that  $R_0$  is a constant set by the choice of system

parameters and physical characteristics (1) of the given burst. From the above it is clear that for a given burst a different choice of bit rate  $R$  yields different number of transmitted bits,  $N_B$ . To find the bit rate  $R_B$  that maximizes  $N_B$  we simply set its derivative with respect to  $R$  to zero and solve

$$\frac{dN_B}{dR} = 0 = \ln(R_0/R) - 1 \quad (3.4.2-3)$$

or  $R_B^* = R_0/e$  where  $e$  is the natural logarithm base. Using the last result in eq (3.4.2-2) yield  $N_B^*$  the maximum number of bits for this burst.

$$N_B^* = \frac{R_0 \cdot B}{e} \quad (3.4.2-4)$$

where  $R_0 = C_u q^2 / N_0 g^{-1}(P_{bmax})$

From the above we see that  $P_{min}^*$  the minimum power corresponding to  $R_B^*$  is equal to  $P(0)/e$ . This implies that the burst duration (transmission time) i.e. the time it takes to drop to  $P_{min}^*$  from  $P(0)$  is equal to one decay time constant  $B$ . Equivalently, then, the above analysis states that for a given bit rate  $R$  the optimal time of transmission  $T_B^*$  must be set to  $B$  to yield the above maximum transmitted bit  $N_B^*$ . This result has been demonstrated by Ables' work [11] as well.

### Variable Bit Rate System

For the given underdense burst we have  $P_b(t) = P_{bmax}$  for all bits. Under such conditions the variable bit rate  $R(t)$  is given by

$$R(t) = R_0 e^{-t/B} \quad (3.4.2-5)$$

$$\text{where } R_0 = C_u q^2 / g^{-1}(P_{bmax})$$

Note that the power to transmission rate ratio which specifies the bit energy is constant and hence the BER is maintained constant.

Since the burst is assumed to be known a-priori we can compute the bit duration (inverse of bit rate) for each bit exactly such that the integral of power received over the individual bit duration i.e. the bit energy is the same for all transmitted bits. See Fig. 13.

The number of bits for variable rate is given by

$$N_{BV} = \int_0^{\infty} R(t)dt = R_0 \cdot B \quad (3.4.2-6)$$

### Comparison of the Two Systems

We now compare constant bit rate system using the optimal  $R$  (with  $BER < P_{bmax}$ ) for the particular burst versus variable bit rate which mimics the bursts power behavior (such that all bits possess the same  $BER$ ,  $P_{bmax}$ ). For each of the above we found the number of bits transmitted  $N^*_B$  and  $N_{BV}$  respectively. Taking the ratio:

$$N_{BV}/N^*_B = e$$

We see an improvement of 2.7 for the utilization of variable bit rate over constant bit rate. We stress however that the necessary priori knowledge (or estimation) of burst characteristics is unreliable. In addition, although variable bit rate results in a higher number of transmitted bits for a given burst versus constant bit rate there is a price; all bits have a  $BER = P_{bmax}$  for variable bit rate system whereas for the constant bit rate system  $P_{bmax}$  is a worst case

(last bit BER). This fact portends worse probability of correct packet transmission for variable rate system than constant rate system under the above conditions.

### 3.4.3 Throughput for Constant Bit Rate

We are given a communication system with a specified maximum allowed BER  $P_{bmax}$ , constant transmission rate  $R$ , received noise power spectral density  $N_0$  and general system parameters (link distance, frequency, etc.) as defined by  $C_U$  or  $C_O$ .

To express the throughput  $T$  of the system we introduce  $N_{Bi}$  as the number of bits transmitted on the  $i$ th burst and  $M_r$  as the number of bursts occurring in the period of  $r$  seconds. Since the bursts are independent of each other, and assuming no overlap of bursts, we have:

$$\begin{aligned}
 T &= \lim_{r \rightarrow \infty} \frac{1}{r} \sum_{i=1}^{M_r} N_{Bi} & (3.4.3-1) \\
 &= A \cdot \bar{N}_B
 \end{aligned}$$

where  $A$  is the average number of bursts/s and  $N_b$  is the expected number of bits per burst as averaged over the ensemble of all bursts' profiles. (The subscripts U or O are added to distinguish between underdense and overdense cases.)

For underdense:

$$N_{bu} = \int \int N_b(q, B) f_q(q) f_B(b) dq db \quad (3.4.3-2)$$

where  $f_x ()$  is the pdf of  $x$ .

For overdense:

$$N_{bo} = \int N_b(q) f_q(q) dq \quad (3.4.3-3)$$

Note that the above three equations are dependent on the choice of bit rate  $R$ .

#### 3.4.3.1 Optimal Average Throughput for Constant Bit Rate System -- Underdense.

In this section the optimal average system throughput for the underdense burst is given. This is the maximum average number of bits per unit time

for the 'best' transmission rate  $R$  (and other system constants) assuming only underdense bursts are present.

This optimal throughput is found by first deriving the dependence of the average throughput (Eq. 3.4.3-1) on the bit rate  $R$ , and solving for the optimal bit rate  $R^*$  that would yield the desired optimal throughput  $T^*$ . The solution is done with respect to the normalized bit rate,  $R_N$ , which yields a result independent of a particular choice of system values.

For the given system  $P_{bmax}$ ,  $N_0$ ,  $R$  and  $C_U$  are specified. We have defined  $R_N$  the normalized bit rate as:

$$R_N = \frac{R}{R_{max}} = \left( \frac{q_{min}}{q_U} \right)^2$$

where

$$R_{max} = \frac{C_U q_U^2}{N_0 g^{-1}(P_{bmax})} \quad (3.4.3.1-1)$$

the maximum bit rate achievable in a given system using underdense bursts.

Omitting the cumbersome derivation we present the following results: (for the relevant derivation see Sec. 4.2)

The average number of bits per underdense burst  $N_{bu} = R \cdot \bar{T}_b$  can be expressed in terms of the normalized bit rate using Eq. (3.4.1.1-3) as:

$$N_{bu} = \frac{2\bar{B}}{p-1} R_{max} \frac{1}{1-R_N^{p'}} [R_N - R_N^{p'+1} + R_N^{p'+1} \cdot \ln(R_N^{p'})] \quad (3.4.3.1-2)$$

where

$p' = (p - 1)/2$ ,  $p=1.6$  and  $R_{max}$  is defined above.

Note that in the above expression the bursts considered were those with an electron line density  $q$  between  $q_{min}$  (as defined by  $P_{min}$ ) and  $q_U$  (the physical limit). The arrival rate for such condition is given by Eq. (2.3-2) where  $q_1$  is set to  $q_{min}$  and  $q_2$  is  $q_U$ . Together with Eq. (3.4.3.1-1) we have for the arrival rate of underdense bursts:

$$A_U = A' \cdot \left[ \frac{1}{\sqrt{R_N}} - 1 \right] \quad (3.4.3.1-3)$$

where,

$$A' = \frac{19.1667 \cdot \phi \sin \phi (R_R \zeta)^2}{q_U}$$

$$q_U = 10^{14}$$

The expression for throughput using underdense bursts is given by the product of the last two Eqs. as specified by Eq. (3.4.3-1). The result is a function of the normalized bit rate which is just a scaled bit rate. In the product we substitute for  $R_{\max}$  from Eq. (3.4.3.1-1) and for  $C_U$  and  $B$  from Eq. (2.1.1-2). For a given set of system parameters we thus have the throughput (using underdense bursts) for any choice of (normalized) bit rate as:

$$T_U = 3.056 \cdot 10^{-19} \cdot \frac{P_T G_T G_R \zeta^2 \phi \sin \phi \sec^2 \phi \exp\left(-\frac{33.359}{\lambda^2 \sec^2 \phi}\right) \cdot \lambda^5}{(p-1) N_0 \cdot g^{-1}(P_{b_{\max}}) \cdot D \cdot R_T} \cdot \frac{\sqrt{R_N} - R_N}{1 - R_N^p} [1 - R_N^p + p \cdot R_N^{p-1} \cdot \ln(R_N)] \quad (3.4.3.1-4)$$

where

- $p$  is an empirical constant ,  $p'=(p-1)/2$   
(taken here as 1.6, Section 2.1.2)
- $\zeta$  idealized antenna beamwidth.
- $R_T$  and  $\phi$  geometric parameters determined  
by link distance (from section 2.2)
- $P_T$  transmitter power.
- $G_T, G_R$  transmitter and receiver antenna gains.
- $\lambda$  carrier wavelength.
- $D$  diffusion coefficient of the atmosphere.
- $N_0$  power spectral density of the noise.  
(Sec. 2.4)
- $g^{-1}(P_{bmax})$  ratio of minimum bit energy to  $N_0$ .

Note that the equation is written in two parts; the first incorporates all the parameters of the particular system and the second part reflects the variation in throughput with choice of bit rate. The above throughput (divided by about 3200 bits/s) for our sample system (defined in Sec. 3.3) is plotted in Fig. 16. Note the maximum is 214 b/s.

We would like to find from the above equation the optimal normalized bit rate  $R_N^*$  which yields the

maximum throughput  $T_U^*$ . This optimal normalized bit rate for any given system is found numerically to be (see Fig. 16):

$$R_N^* = .07$$

or equivalently the optimal bit rate,

$$R^* = .07 R_{\max} \quad (3.4.3.1-5)$$

resulting in

$$T_U^* = 3.433 \cdot 10^{-20} \cdot \frac{P_T G_T G_R \zeta^2 \phi \sin(\phi) \sec^2(\phi) \exp\left(-\frac{33.359}{\lambda^2 \sec^2 \phi}\right) \lambda^5}{R_T N_0 g^{-1}(P_{b\max}) D} \quad (3.4.3.1-6)$$

where all the parameters are defined above.

The above expression for the maximum throughput  $T_U^*$  allows us to quantify the affects of various system parameters and constraints on the best throughput using a constant bit rate. As an example we plotted the variation of  $T_U^*$  as a function of wavelength for our sample system (Sec 3.3). See Fig. 17 bottom

curve. Using our sample system with a wavelength of 6 m. (50 MHz) we get  $R_{\max} = 86.5$  kb/s,  $R^* = 6.055$  kb/s and  $T_U^* = 214$  b/s.

#### 3.4.3.2 Optimal Average Throughput for Constant Bit Rate System -- Overdense.

In this section the optimal average system throughput for the underdense burst is given. This is the maximum average number of bits per unit time for the 'best' transmission rate  $R$  (and other system constants) assuming only overdense bursts are present.

This optimal throughput is found by first deriving the dependence of the average throughput (Eq. 3.4.3-1) on the bit rate  $R$ , and solving for the optimal bit rate  $R^*$  that would yield the desired optimal throughput  $T_O^*$ . The solution is done with respect to the normalized bit rate,  $R_{NO}$ , which yields a result independent of a particular choice of system values.

For the given system  $P_{bmax}$ ,  $N_0$ ,  $R$ ,  $a$  and  $C_0$  are specified. With a reference to Eq. (3.4.1.2-3) and the accompanying discussion we rewrite  $R_{NO}$  -- the bit rate normalized with respect to  $R_{maxo}$ , the maximum bit rate achievable for the given system using overdense bursts -- and related parameters:

$$q_T = q_{uo} \cdot R_{NO}^2$$

$$R_{NO} = \frac{R}{R_{maxo}}$$

$$R_{maxo} = \frac{C_0 \sqrt{a \cdot q_{uo}}}{\sqrt{e \cdot N_0 \cdot g^{-1}(P_{bmax})}}$$

$$q_{mino} = \max\{q_T, q_{LO}\}$$

(3.4.3.2-1)

where,  $q_{uo} = 10^{16}$  and  $q_{LO} = 10^{14}$

$a$  and  $C_0$  are defined in Eq. (2.1.5-2).

$N_0$  is defined in Sec. 2.4

We note from the above that for  $q_T < q_{LO}$  (or equivalently  $R_{NO} < .1$ ) where  $q_{mino} = q_{LO}$  and the other for  $q_T > q_{LO}$  (or equivalently  $R_{NO} > .1$ ) where  $q_{mino} = q_T$ . In addition, the value of  $Q$  (Eq. (3.4.1.2-3)) varies with the  $R_{NO}$  as well since  $Q$  is

a function of  $q_{\text{mino}}$  - see Eq. (2.1.6-2). For the case where  $R_{\text{NO}} > .1$  ( $q_{\text{T}} > q_{\text{LO}}$ ) we have

$$Q = .5(q_{\text{UO}})^{.5} R_{\text{NO}} / (1-R_{\text{NO}})$$

For the case where  $R_{\text{NO}} < .1$  ( $q_{\text{T}} > q_{\text{LO}}$ ) we have

$$Q = .5(q_{\text{LO}})^{.5} / .9$$

Using the above relationships in Eq. (3.4.1.2-3) to express the average overdense burst duration as a function of  $R_{\text{NO}}$  we get:

For  $R_{\text{NO}} \leq 0.1$  :

$$i_{\text{B}} = \sqrt{q_{\text{LO}}q_{\text{UO}}}\alpha \cdot R_{\text{NO}} \left\{ \sqrt{\frac{1}{R_{\text{NO}}^2} - 1} - \sqrt{\frac{0.01}{R_{\text{NO}}^2} - 1} + \cos^{-1}(10R_{\text{NO}}) - \cos^{-1}(R_{\text{NO}}) \right\}$$

(3.4.3.2-2)

For  $R_{\text{NO}} > 0.1$  :

$$i_{\text{B}} = .95\sqrt{q_{\text{LO}}q_{\text{UO}}}\alpha \cdot R_{\text{NO}} \left\{ \sqrt{\frac{1}{R_{\text{NO}}^2} - 1} - \cos^{-1}(R_{\text{NO}}) \right\}$$

The average number of bits per overdense burst is by definition

$$\bar{N}_{\text{BO}} = R \cdot \bar{i}_{\text{B}} \quad (3.4.3.2-3)$$

and can be expressed in terms of the normalized bit rate using Eq. (3.4.3.2-1) for  $R$  as a function of  $R_{\text{NO}}$

and Eq. (3.4.3.2-2) for the average overdense burst duration.

Since the throughput  $T_0$  according to Eq. (3.4.3-1) is the product of the arrival rate and the last equation i.e.

$$T_0 = A_0 \cdot \bar{N}_{BO} \quad (3.4.3.2-4)$$

we need to express the arrival rate of overdense bursts  $A_0$  as a function of  $R_{NO}$ . We start by employing Eq. (2.3-2) with  $q_1$  set to  $q_{\text{mino}}$  (the lowest overdense  $q$  as determined from the choice of  $P_{\text{min}}$  i.e. bit rate) and  $q_2$  set to  $q_{\text{UO}}$  (the physical maximum). The dependence of  $q_{\text{mino}}$  on  $R_{NO}$  is then used (discussed above after Eq. (3.4.3.2-1)) yielding the following arrival rate:

$$A_0 = \left\{ \begin{array}{ll} .99 \cdot A' & R_{NO} \leq .1 \\ .01 \cdot A' \left[ \frac{1}{R_{NO}^2} \right] & R_{NO} > .1 \end{array} \right\} \quad (3.4.3.2-5)$$

where,

$$A' = \frac{3 \cdot \phi \sin \phi (R_R \zeta)^2}{q_{LO}}$$

$$q_{UO} = 10^{16} \quad \text{and} \quad q_{LO} = 10^{14}$$

By direct substitutions from the above equations we express the throughput using overdense bursts as a function of normalized bit rate and system parameters as:

$$T_o = .33 \cdot 10^{10} \cdot \frac{P_T G_T G_R \zeta^2 \phi \sin \phi \sec^3 \phi \cdot \lambda^3}{N_0 \cdot g^{-1}(P_{bmax}) \cdot D \cdot R_T}$$

$$\left\{ \begin{array}{l} 11 R_{NO}^2 \left\{ \sqrt{\frac{1}{R_{NO}^2} - 1} - \sqrt{\frac{0.01}{R_{NO}^2} - 1} + \cos^{-1}(10 R_{NO}) - \cos^{-1}(R_{NO}) \right\} \quad R_{NO} \leq .1 \\ \frac{R_{NO} - R_{NO}^3}{1 - R_{NO}} \left\{ \sqrt{\frac{1}{R_{NO}^2} - 1} - \cos^{-1}(R_{NO}) \right\} \quad R_{NO} > .1 \end{array} \right\}$$

(3.4.3.2-6)

where,

- $\zeta$  idealized antenna beamwidth.
- $R_T$  and  $\phi$  geometric parameters determined by link distance (from section 2.2)
- $P_T$  transmitter power.
- $G_T, G_R$  transmitter and receiver antenna gains.
- $\lambda$  carrier wavelength.
- $D$  diffusion coefficient of the atmosphere.
- $N_0$  power spectral density of the noise.  
(Sec. 2.4)
- $g^{-1}(P_{bmax})$  minimum of bit energy to  $N_0$  ratio.

Note that the equation is written in two parts; the first incorporates all the parameters of the particular system and the second part reflects the variation in throughput with choice of bit rate. The above throughput (multiplied by 2.55) for our sample system (Sec 3.3) is plotted in Fig. 18.

We would like to find from the above equation the optimal normalized bit rate  $R_{NO}^*$  which yields the maximum throughput  $T_O^*$ . This optimal normalized bit rate for any given system is found numerically to be (see Fig. 18):

$$R_{NO}^* = .1$$

or equivalently the optimal bit rate,

$$R^* = .1 R_{maxo} \quad (3.4.3.1-7)$$

The result is intuitively obvious since  $R_{NO}=.1$  is the maximum bit rate that still includes all overdense trails i.e maximum arrival rate. For a higher bit rate we have a smaller arrival rate that reduces the throughput. A smaller bit rate will not change the overdense arrival rate but will diminish the throughput.

Using the optimal bit rate for overdense bursts we get the maximum overdense throughput  $T_0^*$  by substituting Eq.(3.4.3.2-7) into Eq. (3.4.3.2-6) yielding:

$$T_0^* = .3078 \cdot 10^{-18} \cdot \frac{P_T G_T G_R \zeta^2 \phi \sin \phi \sec^3 \phi \cdot \lambda^5}{N_0 \cdot g^{-1}(P_{bmax}) \cdot D \cdot R_T} \quad (3.4.3.2-8)$$

where all the parameters are defined above.

The above expression for the maximum throughput  $T_0^*$  allows us to quantify the affects of various system parameters and constraints (wavelength, power, link distance, maximum bit error rate etc.) on the best throughput using a constant bit rate. Using our sample system (Sec 3.3) with a wavelength of 6 m. (50 MHz) we get  $R^* = 252$  kb/s and  $T_0^* = 8688$  b/s.

### 3.4.3.3 Total Average Throughput for Constant Bit Rate System.

In this section we combine the result of the last two sections to present the total throughput and optimal throughput. Since we used differently normalized variables for underdense and overdense we shall now employ a single normalized variable; the one corresponding to the overdense case.

Recalling previous definitions:

For underdense we used

$$R_N = \frac{R}{R_{max}} = \left( \frac{q_{min}}{q_U} \right)^2$$

where

$$R_{max} = \frac{C_U q_U^2}{N_0 g^{-1}(P_{bmax})} \quad (3.4.3.3-1)$$

the maximum bit rate achievable in a given system using underdense bursts.  $C_U$  and  $N_0$  are defined in Eq. (2.11-2) and Eq. (2.4-2), respectively.

For overdense we used

$$R_{NO} = \frac{R}{R_{maxo}}$$

where

$$R_{maxo} = \frac{C_o \sqrt{a \cdot q_{uo}}}{\sqrt{e \cdot N_0 \cdot g^{-1}(P_{bmax})}} \quad (3.4.3.3-2)$$

where,  $q_{UO} = 10^{16}$  and  $q_{LO} = 10^{14}$   
 $a$  and  $C_0$  are defined in Eq. (2.1.5-2).  
 $N_0$  is defined in Sec. 2.4

From the above we can write

$$\frac{R_{maxo}}{R_{max}} = s = 6.446 \cdot e^{(33.359/\lambda^2 \sec^2 \phi)} \cdot \sec \phi \quad (3.4.3.3-3)$$

and

$$R_N = s \cdot R_{NO} \quad (3.4.3.3-4)$$

Note that  $R_N=1$ , the maximum underdense bit rate, corresponds to  $R_{NO} = 1/s$ .

Using Eq. (3.4.3.1-4) for the underdense throughput, with  $R_N$  expressed by the last equation, and Eq. (3.4.3.2-6) for the overdense throughput we get for the total throughput  $T$ :

$$T = .509 \cdot 10^{-18} \cdot \frac{P_T G_T G_R \zeta^2 \phi \sin \phi \sec^2 \phi \cdot \lambda^5}{N_0 \cdot g^{-1}(P_{bmax}) \cdot D \cdot R_T} \cdot \{T_U + T_{O1} + T_{O2}\} \quad (3.4.3.3-5)$$

where

$$T_U = \exp\left(-\frac{33.359}{\lambda^2 \sec^2 \phi}\right) \frac{\sqrt{s R_{NO}} - s R_{NO}}{1 - (s R_{NO})^p} \left[ 1 - (s R_{NO})^p + p (s R_{NO})^p \cdot \ln(s R_{NO}) \right] \cdot U\left(\frac{1}{s} - R_{NO}\right)$$

$$T_{O1} = \frac{\sec \phi R_{NO}^2}{.1401} \left[ \sqrt{\frac{1}{R_{NO}^2} - 1} - \sqrt{\frac{0.01}{R_{NO}^2} - 1} + \cos^{-1}(10 R_{NO}) - \cos^{-1}(R_{NO}) \right] \cdot U(.1 - R_{NO})$$

$$T_{O2} = .649 \cdot \sec \phi \cdot \frac{R_{NO} - R_{NO}^3}{1 - R_{NO}} \left[ \sqrt{\frac{1}{R_{NO}^2} - 1} - \cos^{-1}(R_{NO}) \right] \cdot U(R_{NO} - .1)$$

$$s = 6.446 \cdot e^{(33.359/\lambda^2 \sec^2 \phi)} \cdot \sec \phi$$

and

$$U(x) = \begin{cases} 1 & \text{for } x \geq 0 \\ 0 & \text{for } x < 0 \end{cases}$$

is the unit step function.

All other parameters are defined in previous sections.

### 3.5 Variable Bit Rate and Constant BER System

#### 3.5.1 Channel Duration

For a variable bit rate system the bit rate is

changed so as to maintain a reasonably constant energy per bit. Clearly it implies a constant BER,  $P_b$ , for all transmitted bits. Considering for example the underdense burst, if apriori knowledge of the burst were available, we could divide the received power curve into equal energy portions and compute the resulting individual bit durations before we transmit. Under such conditions all bits will possess exactly the same energy and hence the same BER. The total number of bits transmitted for that burst will simply be proportional to the total area under the received power-versus-time curve. Since we don't have an apriori knowledge of the burst but rather an instantaneous (within a negligible delay) indication of channel strength we can only evaluate the necessary duration for the current bit and transmit it as such. During the duration of the transmitted bit the power received drops. If the bit duration is small the resulting drop in bit energy is negligible and our assumption of constant bit energy is not violated. As time progresses, however, the bit duration increases (power received decays) and the drop in bit energy relative to the assumed constant bit energy becomes appreciable and

finally intolerable. This fact limits the maximum bit duration which in turn restricts the duration of transmission or, equivalently, channel duration.

### 3.5.1.1 Transmission Duration for Variable Bit Rate -- Underdense

We start by imposing our fidelity constant,  $k$ , for the normalized bit energy -- the ratio of the real bit energy to the desired one. For our derivation we will assume  $k > .9$  i.e. no more than 10% drop in bit energy shall be tolerated. We further define:

$P_b$	Assumed constant BER for all transmitted bits.
$T_{bi}$	Duration of the $i^{\text{th}}$ bit
$R(t)$	Instantaneous bit rate
$T_0$	Duration of the first bit, $1/R_0$
$N$	Last bit
$T(m)$	Total duration of the first $m$ bits; also starting time of the $(m+1)^{\text{th}}$ bit:

$$\sum_{i=1}^m T_{bi}$$

- $T_t$  Duration of transmission (burst duration) =  
 $T(N)$
- $c$  Max ( $T_{bN}/B$ ) for a given  $k$ .

In order to maintain a constant BER,  $P_b$ , we have for the variable bit rate

$$R(t) = \frac{C_U q^2}{N_0 g^{-1}(P_b)} e^{-t/B} = R_0 \cdot e^{-t/B} \quad (3.5.1.1-1)$$

and the  $n^{\text{th}}$  bit duration is given by

$$T_{bn} = T_0 e^{\frac{T(n-1)}{B}} \quad (3.5.1.1-2)$$

where

$$T_0 = 1/R_0 = N_0 g^{-1}(P_b)/C_U q^2$$

For  $k > .9$  we have for the last bit,  $N$ :

$$T_{bN} \leq [1.5 - \sqrt{2.25 - 6(1-k)}] \cdot B = c \cdot B \quad (3.5.1.1-3)$$

Combining with eq (3.5.1.1-2) we have

$$\frac{T_{bN}}{B} = \frac{T_0}{B} \cdot e^{\frac{T(N-1)}{B}} \leq c \quad (3.5.1.1-4)$$

Since the transmission duration is given by

$$T_t = T(N-1) + T_{bN} \quad \text{we have from the last}$$

3 eqns.

$$T_t \leq B \cdot [c + \ln\left(\frac{c \cdot B}{T_0}\right)] \quad (3.5.1.1-5)$$

for  $k = .9$ ,  $c = .2$  we have from the above  $T_t/B = .2 + \ln(R_0B/5)$ .

For all practical systems we can safely use

$$T_t = B \cdot \ln\left(\frac{R_0 \cdot B}{5}\right) \quad (3.5.1.1-6)$$

where  $R_0$  is defined in Eq. (3.5.1.1-1)

### 3.5.2 Throughput for Variable Bit Rate System

#### - Underdense

Using the results from the previous section on transmission duration we can find the approximate number of transmitted bits by integrating  $R(t)$  from time 0 to time  $T_t$ :

$$N_{BU} = R_0 B = C_U B q^2 / g^{-1}(P_b) N_0$$

(3.5.2-1)

where  $R_0$  is the variable bit rate at time 0.

and since  $B$  and  $q$  are independent the average of  $N_{UV}$  over the joint space of  $q$  and  $B$  yields:

$$N_{uv} = \frac{C_u \overline{Bq^2}}{g^{-1}(P_b) \cdot N_0} \quad (3.5.2-2)$$

The derivation of the above equations is in section 4.5

We shall assume that the bit rate shall vary between  $R_{minV}$  and  $R_{maxV}$ . Bearing in mind that for a given bit rate  $R$  we have a corresponding  $q$  such that

$$C_u q^2 = N_0 \cdot g^{-1}(P_b) \cdot R \quad q_L < q < q_U \quad (3.5.2-3)$$

As a result we have

$$q_{minV} = \sqrt{\frac{N_0 \cdot g^{-1}(P_b)}{C_u}} \cdot \sqrt{R_{minV}} \quad (3.5.2-4)$$

$$q_{maxV} = \sqrt{\frac{N_0 \cdot g^{-1}(P_b)}{C_u}} \cdot \sqrt{R_{maxV}} \quad (3.5.2-5)$$

$R_{minV}$  must be chosen such that  $q_{minV} > q_L$ , the physical minimum.

$R_{maxV}$  must be chosen such that  $q_{maxV} < q_U$ , the physical maximum.

Note that because our empirical arrival rate relationship (Sec. 2.3) is valid for  $q > 10^{13}$  we shall set  $R_{minV}$  such that  $q_{minV} > 10^{13}$ .

To get the most throughput out of our system we set

$R_{\max V}$  to its maximum value i.e. corresponding to  $q=q_U$ . We thus have set  $q_{\max V}=q_U$  and using it in the last two equations we have

$$\frac{q_{\min V}}{q_{\max V}} = \frac{q_{\min V}}{q_U} = \sqrt{\frac{R_{\min V}}{R_{\max V}}} = \sqrt{R_{NV}} \quad (3.5.2-6)$$

where  $R_{\max V}$  is given by Eq.(3.5.2-5) as

$$R_{\max V} = \frac{C_U q_U^2}{N_0 g^{-1}(P_b)} \quad (3.5.2-7)$$

where,  $C_U$  is from Eq.(2.1.1-2),  $N_0$  is from (2.4-2) resulting in Eq.(3.5.2-13).

Note that  $R_{\max V} = R_{\max}$  the maximum underdense for constant bit rate system if we set  $P_b=P_{b\max}$ , a direct result from Eq. (3.4.3.1-1)

Evaluating  $E(q^2)$  for Eq. (3.5.2-2) in the range of  $q_{\min V}$ ,  $q_U$  is done using eq (2.12-2)

$$\overline{q^2} = \frac{(p-1)}{(3-p)} q_{\min V}^{p-1} q_U^{3-p} \frac{(1-y^{3-p})}{(1-y^{p-1})} \quad (3.5.2.-8)$$

where  $p=1.6$  and (with Eq. (3.5.2-6))

$$y = \frac{q_{\min V}}{q_U} = \sqrt{R_{NV}}$$

Rewriting we get for the last equation

$$\bar{q}^2 = \frac{.6}{1.4} q_u^2 \frac{(R_{NV}^3 - R_{NV})}{(1 - R_{NV}^3)} \quad (3.5.2-9)$$

Substituting into Eq. (3.5.2-2) we get

$$N_{UV} = \frac{C_U \bar{B}}{g^{-1}(P_b) \cdot N_0} \cdot \frac{.6}{1.4} q_u^2 \frac{(R_{NV}^3 - R_{NV})}{(1 - R_{NV}^3)} \quad (3.5.2-10)$$

For throughput expression we need to have the arrival,  $A_V$ , expressed as a function of our variable  $R_{NV}$ . From Eq. (2.3-2) we have

$$A_V = \frac{A'_V}{q_{minV}} \left( 1 - \frac{q_{minV}}{q_U} \right) = \frac{A'_V}{q_U} \left( \frac{1}{\sqrt{R_{NV}}} - 1 \right) \quad (3.5.2-11)$$

where

$$A'_V = 19.1667 \cdot \sin \phi (R_R \zeta)^2$$

The expression for the throughput,  $T_{UV}$  is dictated by Eq. (3.4.3-1) and is arrived at by the product of Eq. (3.5.2-11) and Eq. (3.5.2-10) above. Using the definitions of Eq. (2.1.1-2) and Eq. (3.5.2-7) we get

$$T_{UV} = 6.54821 \cdot 10^{-20} \cdot \frac{P_T G_T G_R \zeta^2 \phi \sin(\phi) \sec^2(\phi) \exp\left(-\frac{33.359}{\lambda^2 \sec^2 \phi}\right) \lambda^5}{R_T N_0 g^{-1}(P_b) D}$$

$$\left( \frac{1}{\sqrt{R_{NV}}} - 1 \right) \frac{(R_{NV}^3 - R_{NV})}{(1 - R_{NV}^3)} \quad (3.5.2-12)$$

where, (Eq. (3.5.2-7) , Eq. (2.1.1-2) and (2.4-2))

$$R_{maxV} = 2.518 \cdot 10^{16} \cdot \frac{P_T G_T G_R \lambda^3 \exp\left(-\frac{33.359}{\lambda^2 \sec^2 \theta}\right)}{(.063 \lambda^{2.3} + 1) \cdot g^{-1}(P_b) \cdot R_T^3} \quad (3.5.2-13)$$

$R_{NV}$   $R_{minV}/R_{maxV}$  ;  $R_{maxV}$  defined in Eq. (3.5.2-7)

$R_{minV}$  is arbitrary yet if resulting  $R_{NV}$  is small system complexity and cost increases.

$\zeta$  idealized antenna beamwidth.

$R_T$  and  $\theta$  geometric parameters determined by link distance (from section 2.2)

$P_T$  transmitter power.

$G_T, G_R$  transmitter and receiver antenna gains.

$\lambda$  carrier wavelength.

$D$  diffusion coefficient of the atmosphere.

$N_0$  power spectral density of the noise.

(Sec. 2.4)

$g^{-1}(P_{bmax})$  minimum of bit energy to  $N_0$  ratio.

For our sample system (Sec. 3.3) we chose  $R_{minV}=1000$  b/s i.e  $q_{minV} = 1.1 \cdot 10^{13}$ ,  $g^{-1}(P_b)=9$  we get  $R_{NV}=.011558$

and  $T_{UV}$  about 1150 b/s.

If we assume the constant bit energy of the variable rate system to be the same as the minimum bit energy of the constant rate system then for our sample system (underdense only) we improved the throughput from 214 (Sec. 3.4.3.1) to 1150 - a ratio of 5.3.

### 3.5.3 Throughput for Variable Bit Rate System

#### - Overdense

The maximum power point of an overdense burst  $P_{max}$  is well approximated by (Eq. (2.1.5-2) neglecting  $k$ )

$$P_{max} = C_0 \sqrt{\frac{a \cdot q}{e}} \quad (3.5.3-1)$$

We recall that for our variable rate system the rate varies as the power scaled by the bit energy  $N_0 g^{-1}(P_b)$ . This variation in time can be approximated as a triangle whose base lies on time axis from the origin to the point given by  $aq$  and whose top vertex is at  $P_{max}/N_0 g^{-1}(P_b)$ .

Since the number of bits sustained by this overdense

burst,  $N_{bv}$ , is theoretically equal to the area underneath the rate time function we have

$$N_{bv} = \frac{1}{2} \frac{P_{max}}{N_0 g^{-1}(P_b)} \cdot a \cdot q = \frac{1}{2\sqrt{e}} \frac{C_0 a^{3/2}}{N_0 g^{-1}(P_b)} \cdot q^{3/2} \quad (3.5.3-2)$$

Averaging over the ensemble of overdense bursts using Eq. (2.1.6-2) with  $q_{mino}=q_{LO}=10^{14}$  ( $q_{LO}/q_{UO} = .01$ ) we get

$$\overline{q^{3/2}} = \frac{1}{2} q_{UO} \sqrt{q_{LO}} \left( 1 + \sqrt{\frac{q_{LO}}{q_{UO}}} \right) \quad (3.5.3-3)$$

which yields for average number of bits

$$\overline{N}_{ov} = \frac{1}{4\sqrt{e}} \frac{C_0 a^{3/2}}{N_0 g^{-1}(P_b)} \cdot q_{UO} \sqrt{q_{LO}} \left( 1 + \sqrt{\frac{q_{LO}}{q_{UO}}} \right) \quad (3.5.3-4)$$

and the arrival rate is given by Eq. (2.3-2)

$$\Lambda_v = \frac{3 \cdot \phi \sin \phi (R_R \zeta)^2}{q_{LO}} \left( 1 - \frac{q_{LO}}{q_{UO}} \right) \quad (3.5.3-5)$$

Combining all of the above for the throughput expression (variable rate and overdense bursts) we get

$$T_{ov} = 94.686 \cdot 10^{-20} \frac{P_T G_T G_R \zeta^2 \phi \sin \phi \sec^3 \phi \cdot \lambda^5}{N_0 \cdot g^{-1}(P_b) \cdot D \cdot R_T} \quad (3.5.3-7)$$

For our sample system (Sec. 3.3) we get a throughput of 26.7 kb/s.

If we assume the constant bit energy of the variable rate system to be the same as the minimum bit energy of the constant rate system then for our sample system (Sec 3.3) (assuming overdense only) we improved the throughput from 8688 b/s (Sec. 3.4.3.2) to 26.7 kb/s - an improvement ratio of 3.

#### 3.5.4 Comparison of Throughput for Constant and Variable Bit Rate Systems

In this section we shall apply the derived relationships in the previous sections to a practical system. The various parameters of interest are computed. The throughput of the system for the optimal constant bit rate is computed and compared with that of throughput of the system using variable bit rate. This comparison will demonstrate the improvement in throughput for variable bit rate. We start by copying

the parameters of the system from Sec. 3.3:

$L$  = 1000 km link distance. From section 2.2  
we have for the next two parameters:

$\sec(\phi)$  = 18.5 and

$R_T = R_R$  = 514 km.

$P_T$  = 1000 w

$G_T$  = 10 dB.

$G_R$  = 10 dB. And for antenna beamwidth we use

$\zeta$  =  $45.84^\circ$  (.8 rad)

$\lambda$  = 6 m. (50 MHz)

$D$  = 8 m<sup>2</sup>/s

$P_{bmax}$  =  $10^{-5}$  Max. BER for constant bit  
rate system.

Using BPSK modulation we get:

$g^{-1}(P_{bmax}) = 9$

$$N_0 = 4 \cdot 10^{-21} \left[ 80 \left( \frac{\lambda}{15} \right)^{2.3} + 2.5 \right] \text{ W/Hz}$$

See discussion above Eq. (2.4-2).

$N_0$  =  $4.89 \cdot 10^{-20}$  at 50 MHz.

For comparison the BER for variable rate system,  $P_b$ ,  
is set equal to  $P_{bmax}$

$R_{minV}$  = 1000 b/s (minimum variable rate allowed)

### Underdense Comparison

The improvement we get for underdense bursts is arrived at under the assumption that the optimal rate is used for the constant bit rate system and for the variable bit rate system some  $R_{\min V}$  is assumed. In addition, we assume that the  $P_b = P_{b\max}$  i.e. the constant bit energy (variable rate) is assumed equal to the minimum allowed bit energy (constant rate system). We thus divide the relevant equations: Eq. (3.5.2-12) and Eq. (3.4.3.1-6) resulting in the improvement  $I_U$

$$I_U = 1.9 \cdot \left( \frac{1}{\sqrt{R_{NV}}} - 1 \right) \frac{(R_{NV}^3 - R_{NV})}{(1 - R_{NV}^3)}$$

where,

$$R_{NV} = \frac{R_{\min V}}{R_{\max V}}$$

$$R_{\max V} = 2.518 \cdot 10^{16} \cdot \frac{P_T G_T G_R \lambda^3 \exp\left(-\frac{33.359}{\lambda^2 \text{sec}^2 \theta}\right)}{(.063 \lambda^{2.3} + 1) \cdot g^{-1}(P_b) \cdot R_T^3} \quad (3.5.2-13)$$

The above is evaluated using the values of our sample system where

$$R_{NV} = R_{\min V} / R_{\max} = 1000 / 86500 = .01156$$

resulting in

$$I_U = 5.38 \quad \text{or about } 7 \text{ dB}$$

### Overdense Comparison

The relevant equations to be used for comparison of throughputs are Eq.(3.5.3-7) and Eq. (3.4.3.2-8) resulting in an improvement of

$$I_0 = T_{OV}/T^*_0 = 3$$

### Discussion

We shall compare now the improvement in throughput of adaptive rate relative to fixed rate systems for underdense in terms of its components; the arrival rate and the average number of bits transmitted per burst. For fixed rate (underdense bursts) we have the following results:

Fixed Rate:

$$R_{\max} = 86.5 \text{ kb/s}$$

Since the normalized optimal bit rate is=.07 we have

$$R^* = .07 R_{\max} = 6.05 \text{ kb/s}$$

For our system we also have

$$\bar{B} = .264 \text{ sec}$$

$$C_v = 3.8 \cdot 10^{-42}$$

From eq 2.4-2 we have:

$$N_0 = 4.89 \cdot 10^{-20}$$

For this rate we can compute some parameters for general interest:

the average number of bits per underdense burst is (from Eq. (3.4.3.1-2)) 1.846 kb/s per burst

$q_{\min} = .26457 \cdot 10^{14} \text{ e/m}$  ( from eq. 3.4.1.1-1 set R to R\*)

Which yields an arrival rate of .116 bursts per sec or equivalently an average inter-arrival time=8.6 s.

The product of the last two results yield a throughput of 214 b/s

Variable Rate

In general the ratio of the bursts' arrival rates of variable bit rate to fixed bit rate system is given by

$$A_V/A^* = .36 \{ (R_{\max}/R_{\min V})^{.5} - 1 \} \quad (\text{Eq. (3.4.3.1-3)})$$

and Eq.(3.5.2-11)

which in our example yields 2.9.

The average number of bits per burst using variable rate is from Eq. (3.5.2-10)

3.328 kb/s per burst.

The ratio of improvement for the average number of bits per burst is

$$3.328/1.846 = 1.8$$

whereas the improvement in arrival rate is

2.9 yielding a total improvement of 5.3

It is interesting to note that the larger improvement is due to the arrival rate. The arbitrary set  $R_{\min V}$ , the minimum rate allowed in adaptive rate system, sets a lower threshold of electron line density,  $q_{\min V}$ , which utilizes bursts that are precluded for the fixed rate system with its higher electron line density threshold  $q_{\min}$ .

#### 4 DERIVATIONS

This chapter supplements the derivations outlined in previous chapter for the results that have thus far been presented.

##### 4.1 Link Geometry

With reference to fig. 6 and the definitions in section 2.2 we have the following relationships:

$$\psi = L/4R_e \quad (4.1-1)$$

$$\gamma = \frac{\pi}{2} + \psi \quad (4.1-2)$$

$$x = 2R_e \sin^2(\psi) \quad (4.1-3)$$

$$y = x \sin(\psi) = 2R_e \sin^3(\psi) \quad (4.1-4)$$

Since it's always true ( $L < 2000$  km) that  $(L/4R_e)^2 \ll 1$  we have

$$\sin^2(\psi) = \psi^2 = \frac{L^2}{16R_e^2} \quad (4.1-5)$$

By the Law of Cosine we have:

$$h^2 + x^2 - 2xh \cos(\gamma) = R_R^2 = R_T^2 \quad (4.1-6)$$

We substitute for  $x$  and  $y$  and  $\sin^2(\psi)$  from eqns. (4.1-3), (4.1-2), (4.1-5) respectively in eqn. (4.1-6) and arrive at the stated result in section 2.2 after some trivial

algebra.

$$R_T = R_R = \sqrt{(h + L^2/8R_s)^2 + L^2/4} \quad (2.2-1)$$

From the figure we also have:

$$\sec^2(\phi) = \frac{R_R^2}{(h+y)^2}$$

which when combined with eqs. (4.1-4), (4.1-5) and (2.2-1)

yields:

$$\sec^2(\phi) = 1 + \frac{L^2}{\left(2h + \frac{L^2}{4R_s}\right)^2} \quad (2.2-2)$$

and thus completing the derivation.

## 4.2 Derivation of Average Burst Duration,

### Constant Bit Rate

This derivation is for the underdense case. We start with equation (3.4.1.1-1) as the expression for  $t_B$ . Since we want to average over the joint space of  $q$  and  $B$  which are statistically independent. The joint pdf is given by the product of the individual pdfs. Because  $B$  acts as a coefficient in the expression for  $t_B$  the two

integrals are separable. (The individual pdfs for  $q$  and  $B$  are from equations (2.1.2-2) and (2.1.3-2,3) respectively.

$$\bar{t}_B^n = 2^n \bar{B}^n \cdot Q \int_{q_{\min}}^{q_{\max}} (\ln(q/q_{\min}))^n \cdot q^{-p} dq \quad (4.2-1)$$

The above integral can be solved by employing the following substitutions:

$$z = (p-1) \ln(q/q_{\min})$$

$$q = q_{\min} e^{z/(p-1)}$$

$$dq = [q_{\min} / (p-1)] e^{z/(p-1)} dz$$

$$\ln^n(q/q_{\min}) = [z/(p-1)]^n$$

Reduces the above to a single integral of the form

$$\bar{t}_B^n = \frac{2^n \bar{B}^n}{(p-1)^n} \cdot \frac{1}{1-x} \cdot \int_0^{\ln(1/x)} z^n e^{-z} dz \quad (4.2-2)$$

where

$$x = \left( \frac{q_{\min}}{q_U} \right)^{p-1} = \left[ \frac{N_0 \cdot R \cdot g^{-1}(P_{bmax})}{C_U q_U^2} \right]^{\frac{p-1}{2}}$$

which can be solved recursively by parts, yielding

$$\bar{t}_B^n = \frac{2^n \bar{B}^n}{(p-1)^n} \cdot \frac{n!}{1-x} \cdot \left\{ 1 - x \sum_{i=0}^n (-1)^i \frac{\ln^i(x)}{i!} \right\}$$

Setting  $n=1$  and  $n=2$  in the above yields the necessary equations for the expected value and variance of  $t_B$  although some wading through algebra is necessary for the

derivation of the variance.

#### 4.3 Burst Duration Constant Bit Rate - Overdense

Since the roots of the overdense power received equation cannot be solved for directly we use a second order approximation. In fact each side of the overdense 'mountain' is fit with a parabola. The parabolas are expanded about the maximum power point. For the left parabola (which approximate the left side) we use the smaller root and subtract it from the larger root of the right parabola (which approximates the right side of the power equation). This difference is the burst duration for the overdense trail. We start by copying eq. (2.1.5-2)

$$P(t) = C_0 \sqrt{(k+t) \cdot \ln\left(\frac{a \cdot q}{k+t}\right)} \quad t \leq aq - k \quad (2.1.5-2)$$

where,

$$C_o = 3.16628610^{-3} \sqrt{D} \frac{P_T G_T G_R \lambda^2}{R_T^3}$$

$$k = .105625/D$$

$$a = 7.14314310^{-17} \cdot \frac{\lambda^2 \sec^2 \phi}{D}$$

We need to solve for the roots  $t_2, t_1$  of the above eq. when  $P$  is set to  $P_{\min}$  since their difference is our transmission interval - burst duration. To do so we first modify the above eq. as:

$$P_N = \sqrt{r \cdot \ln\left(\frac{1}{r}\right)} \quad k/aq \leq r \leq 1 \quad (4.3-2)$$

or equivalently

$$r \ln(r) + P_N^2 = 0 \quad (4.3-4)$$

where

$$P_N = P / C_o (aq)^{1/2}$$

$$r = (k+t)/aq$$

The above will yield the roots  $r_2, r_1$  for  $P=P_{\min}$

Note that the burst duration is defined as

$$t_B = t_2 - t_1 = aq(r_2 - r_1)$$

(4.3-4)

We are now ready to approximate  $r_2 - r_1$  where  $r_1$  is the 'left' root and  $r_2$  the 'right' root. Note that the above eq. has a maximum  $P_N$  of  $1/(e)^{1/2}$  at  $r=1/e$ .

To approximate  $r_1$  we expand  $\ln(r)$  about  $r=1/e$  and substitute the first two terms for  $\ln(r)$  in the last eq resulting in:  $r^2 - (2/e)r + (1/e)P_N^2 = 0$

Solving and using the smaller root we thus approximate  $r_1$  as:

$$r_1 = \frac{1}{e} \cdot (1 - \sqrt{1 - 3P_N^2}) \quad (4.3-5)$$

To approximate  $r_2$  we expand  $r \ln(r)$  about  $r=1/e$  and substitute the first three terms in eq (4.3-3) and solve for the larger root.

$$r_2 = \frac{1}{e} \cdot (1 + \sqrt{2(1 - eP_N^2)}) \quad (4.3-6)$$

$$r_2 - r_1 = \frac{(1 + \sqrt{2})}{e} \cdot \sqrt{1 - eP_N^2} = 0.88 \sqrt{1 - eP_N^2} \quad (4.3-7)$$

A comparison of the above with an iterative solution of the real (without approximation) roots of the eq (4.3-3) and their difference allows us to replace the .88 constant in the last eq. with .95

$$r_2 - r_1 = .95 \text{ root } [1 - e P \text{ sub } N \text{ super } 2]$$

Since the power for which we want to find the roots is  $P_{\min}$  from eqs. (4.3-3) and (4.3-4) we have the desired

approximation for  $t_B$

$$t_B = .95a \cdot q \cdot \sqrt{1 - \frac{eP_{\min}^2}{C_o^2 a} \cdot \frac{1}{q}} \quad (4.3-8)$$

which is the result stated in (3.4.1.2-1).

Note that  $q > q_{\min} = \max(q_T, q_{L0})$ . If  $q_T$  (which is set by  $P_{\min}$  and system parameters reflected in  $C_o$  and  $a$  is less than  $q_{L0}$  than the minimum overdense electron line density,  $q_{\min}$ , is set to the physical minimum overdense electron line density  $q_{L0}$ . On the other hand if  $q_T$  is bigger than  $q_{L0}$  than the overdense trails with electron line density between  $q_{L0}$  and  $q_T$  have zero burst duration and are not "seen" by our system.

For most practical systems which utilize underdense bursts  $P_{\min}$  is such that:

$q_T \ll q_{L0}$  i.e.  $q_{\min} = q_{L0}$  and  $t_B$  is approximated as  $aq$ , ( $q > q_{L0}$ ) and

$$E(t_B) = .95a E(q) = a(q_{u0} q_{L0})^{1/2} = a 10^{15}.$$

Derivation of CDF and PDF:

From eq. (3.4.1.2-1) we note that  $t_B$  is monotonically increasing with  $q$  such that for any  $t_B < t_1$  we have correspondingly a  $q < q_1$ . For  $t_B = t_1$  we have from eq. (3.4.1.2-1) :

$$q_1 = \frac{q_T}{2} \cdot \left( 1 + \sqrt{1 + \left( \frac{t_1}{\tau} \right)^2} \right) \quad (4.3-8)$$

where  $\tau = \alpha q_T / 2 = (e/2)(P_{min}/C_0)^2$

From the above discussion there is a minimum  $t_1$ ,  $t_{1min}$  corresponding to  $q_{mino}$  and a maximum  $t_1$ ,  $t_{1max}$  corresponding to  $q_{uo}$ , the max overdense electron line density. We can now relate the following probability events:

$$\text{Prob}\{t_B \leq t_1\} = \text{Prob}\{q_{mino} \leq q \leq q_1\} \quad t_{1min} \leq t_1 \leq t_{1max} \quad (4.3-9)$$

We get the CDF of  $q$  using eq (2.1.2-2) such that the right hand side of the last eq. becomes

$$Q' [1 - (q_{mino} / q_1)^{p-1}]$$

Eq (4.3-9) then becomes

$$F_{t_B}(t_1) = Q' \left\{ 1 - \left( \frac{q_{mino}}{q_1} \right)^{p-1} \right\} \quad t_{1min} \leq t_1 \leq t_{1max} \quad (4.3-10)$$

Substituting eq (4.3-8) into the above eq. we get the desired eq. (3.4.1.2 -6).

To get eq. (3.4.1.2-7) we simply take the derivative of eq. (3.4.1.2-7)

4.4 Optimal Average throughput for  
constant bit rate - Underdense

Our first objective is to derive eq. (3.4.3.1-2) from section 3.4.2 we know the number of bits per given underdense burst for a given R and a set of specified system parameters is given by

$$N_{BU} = R t_B \quad (4.4-1)$$

Averaging  $N_{BU}$  over the ensemble of underdense bursts ( $q$  and  $B$  independent) is given by

$$\bar{N}_{BU} = R \cdot \bar{t}_B \quad (4.4-2)$$

rewriting the result in Eq. (3.4.1.1.-3) which is derived in Sec. 4.2

$$\bar{t}_B = \frac{2\bar{B}}{p-1} \cdot \frac{1}{1-x} \cdot [1 - x(1 - \ln x)] \quad (3.4.1.1-3)$$

where

$$x = \left( \frac{q_{\min}}{q_U} \right)^{p-1} = \left[ \frac{N_0 \cdot R \cdot g^{-1}(P_{bmax})}{C_U q_U^2} \right]^{\frac{p-1}{2}}$$

and

$$\bar{B} = 3.166 \cdot 10^{-3} \cdot \frac{\lambda^2 \text{sec}^2 \phi}{D} \quad q_U = 10^{14} \quad p = 1.6$$

$$R_N = \frac{R}{R_{\max}} = \left( \frac{q_{\min}}{q_U} \right)^2$$

$$R_{\max} = \frac{C_U q_U^2}{N_0 g^{-1}(P_{b\max})}$$

we substitute for  $x$  and  $R$  in terms of their  $R_N$  definitions and write

$$(R_N)^{p'} = x \quad p' = (p-1)/2 \quad (p = 1.6)$$

$$R = R_N R_{\max}$$

Substituting these into eq. (4.4-2) yields the desired eq. (3.4.3.1-2)

$$N_{BU} = \frac{2\bar{B}}{p-1} R_{\max} \frac{1}{1 - R_N^{p'}} [R_N - R_N^{p'+1} + R_N^{p'+1} \cdot \ln(R_N^{p'})] \quad (3.4.3.1-2)$$

This eq. specifies for a given choice of  $R$  the average number of bits/burst. The rest is in Sec. 3.4.3.1

#### 4.5 Transmission Duration & Throughput for Variable Bit Rate System

With reference to section 3.5.1.1 we define again the following terms:

#### 4.5 Transmission Duration & Throughput for Variable Bit Rate System

With reference to section 3.5.1.1 we define again the following terms:

$P_b$	Assumed constant BER for all transmitted bits.
$T_{bi}$	Duration of the $i^{\text{th}}$ bit
$R(t)$	Instantaneous bit rate
$T_0$	Duration of the first bit, $1/R_0$
$N$	Last bit
$T(m)$	Total duration of the first $m$ bits; also starting time of the $(m+1)^{\text{th}}$ bit:

$$\sum_{i=1}^m T_{bi}$$

$T_t$	Duration of transmission (burst duration) = $T(N)$
$c$	Max $(T_{bN}/B)$ for a given $k$ .

We wish to maintain the actual bit energy above a certain fraction say 90% of the assumed bit energy. This will insure a relatively constant BER corresponding to the assumed bit energy. Since the last bit, the  $N^{\text{th}}$  bit, has

the longest duration (power is monotonically decreasing)  
the loss in bit energy relative to the assumed level is  
the largest. in equation form:

$$E_b \text{ actual} > k E_b \text{ assumed}$$

i.e.

$$\int_0^{T_{bN}} P(T(N-1)) \cdot e^{-t/B} dt \geq k \cdot P(T(N-1)) \cdot T_{bN}$$

which implies

$$1 - kT'_{bN} > \exp(-T'_{bN}) \quad \text{where } T'_{bN} = T_{bN}/B$$

and assuming  $T'_{bN} < 1$  we use the first four terms in the  
series expansion of the exponential (about 0) and get the  
root of  $T'_{bN}$  yielding

The quadratic equation in  $T'_{bN}$  yields

$$T'_{bN} = \frac{T_{bN}}{B} < 1.5 - \sqrt{2.25 - 6(1-k)} = c$$

From the above definitions of the  $N^{\text{th}}$  bit duration we  
have

$$T_{bN}/B = [1/R_0 B] \exp(T(N-1)/B) < c$$

$$\text{yet by definition } T(N-1) = T_t - T_{bN}$$

$$\text{we have then } T_t < B [c + \ln(cR_0B)]$$

which is the result stated in eq. (3.5.1.1-5)

We now evaluate the number of bits for a given burst using variable bit rate as

$$N_{BU} = \int_0^{T_{subt}} R(t) dt = R_0 B \left( 1 - \exp\left(\frac{-T_t}{B}\right) \right)$$

Using the maximum  $T_t$  from eq. (3.5.1.1-4) i.e. letting  $N_B$  = maximum  $N_B$  we have

$$N_{BU} = R_0 B + 1 - 1/c$$

For  $K=.9$   $c=.2$

For all practical system  $R_0 B \gg 4$   
such that

$$N_{BU} = R_0 B = c_u B q^2 / q^{-1}(P_b) N_0$$

as stated in section 3.5.2 Eq. (3.5.2-1)

The average throughput is proportional to the ensemble average of  $N_{BU}$ . Since  $B$  and  $q$  are statistically independent we have

$$N_{BU} = \frac{C_u}{q^{-1}(P_b) \cdot N_0} \cdot B \cdot q^2$$

which is Eq. (3.5.2.-2)

## 5 CONCLUSION AND IDENTIFICATION OF FUTURE WORK

In this work a complex stochastic model for the meteor burst channel was used to serve as the bedrock for the analysis of two different communication systems. The first system assumed we are transmitting with a constant bit rate while the BER is time varying yet constrained to be below some maximum level. The second communications system employs a variable bit rate whose adaptive behavior is controlled so as to maintain constant BER. Both systems operate under the control of a communication feedback protocol that provides knowledge of channel arrival (the instant at which the channel first becomes available) and monitor the strength (power received) of the channel. The research herein focused on throughput and related parameters. The average throughput was shown to depend upon the arrival rate of the bursts and the expected number of bits per burst as averaged over the ensemble of (random) time functions that describe its behavior. In deriving the expressions for the above it was necessary to derive the relationship between the number of bits per given burst and bit rate. This in turn requires understanding of channel duration - the available transmission time - for a given channel (burst).

For constant bit rate system the channel duration decreases with increasing bit rate. Since the number of bits transmitted on the burst is given by the product of burst duration and bit rate a clear tradeoff exists between bit rate and transmission time. This, naturally, implies the existence of an optimal bit rate that would maximize the number of transmitted bits for the burst. Having chosen an optimal bit rate for the burst at hand we must repeat the process for the next burst whose behavior is different. In fact, to optimize the throughput we must change the bit rate from one burst to the next. Having to change the bit rate on a per burst basis, however, requires knowledge of the burst time behavior. The problem with this last requirement is twofold; first, a priori knowledge of the burst is not available and second, estimation of the burst based on assumed ideal behavior is unreliable since the bursts often deviate from such assumed behavior. To counter this limitation we derived the relationship between the constant bit rate and the expected average number of bits per burst since the latter is directly proportional to throughput. We then find the constant bit rate (for the system) which will maximize the throughput. This bit rate is fixed over all bursts and therefore it is a system-optimal bit rate. Having found the maximum average number of bits per burst we multiply by the arrival rate of burst and get the maximum

throughput expression in terms of system parameters and constraints. The significance of such expression is its utility in analyzing/improving existing systems and in designing future constant bit rate meteor burst systems.

In variable bit rate systems we change the bit duration (on a bit by bit basis) so the bit energy remains constant corresponding to our desired fixed BER. The bit energy is given by the time integral of the power received function over the duration of the bit. Finding the individual bit durations is tantamount to dividing the power received curve into equal strips each of area equal to the bit energy. As discussed earlier a priori knowledge of the burst time function is not available and estimation is at best problematic. This precludes exact solution of the bit duration. The best we can do is determine the bit duration based on the bit power at the beginning time of the bit. This may yield an optimistic (too short) bit duration if the power decays during the duration of the bit. The energy per bit for such a case would be below the desired fixed one. If the power is monotonically decreasing there will be a bit whose bit energy relative to the assumed bit energy will be unacceptable. The restriction on maximum bit duration in turn constrains theoretically yet not practically, as has been shown, the total time of transmission for the burst. The number of bits transmitted during a burst can be

approximated by the area under the power received for the interval given by transmission time. The throughput is found by multiplying the arrival rate by the average number of bits per burst.

As it turns out the throughput for variable rate system is about six dB higher for a conservative sample system. The interesting point however is the fact that the improvement of throughput for variable over constant bit rate system (using underdense bursts only) was in large part due to the arrival rate. For constant bit rate system the high optimal bit rate precluded many bursts (those with electron line density below the minimum line density threshold) from being useful resulting in a low arrival rate. For variable rate systems since the bit rate can be quite low (though limited) implies a lower level of cutoff for useful bursts and higher arrival rate. The tradeoff lies in the fact that a low threshold rate for the adaptive rate increase system complexity.

The improvement in throughput however must be kept in perspective. Our analysis assumed that the constant BER under variable rate system is same as the worst BER for the constant bit rate system. Consequently, given  $N$  transmitted bits the probability of all being error free is lower for the constant bit rate than for the variable bit rate system.

The higher throughput for overdense relative to underdense bursts is a natural outcome of its longer average burst duration. The tradeoff, however, is in the much longer inter-arrival time of the overdense bursts compared with underdense; a ratio of 15:1. We see then that for short urgent messages where waiting time is crucial if we are given a constant bit rate system it is advantageous to operate the system at the optimal rate corresponding to underdense burst utilization.

In this analysis many parameters considerations and variables interplay. Amongst them complexity of model, empirical values, transmitter power antenna design link geometry and geographic location, frequency, noise behavior modulation bit rate and BER. All of the above have been integrated and the derived closest form relationships are stated in the most general form incorporating all possible variables to facilitate their usage as design and analysis tools. Furthermore, these expressions define and better delineate the tasks for future analysis. Some of the issues that need be investigated are coding, packet design, modulation protocol development and networking. Each of these requires extensive research and, clearly, there is no 'ultimate' meteor burst system but rather application dependent design. With faster and cheaper hardware for

control and storage and renewed focus on this complex channel it is clear that we are in the exciting phase of using this natural phenomenon for communication.

## 6 TABLES

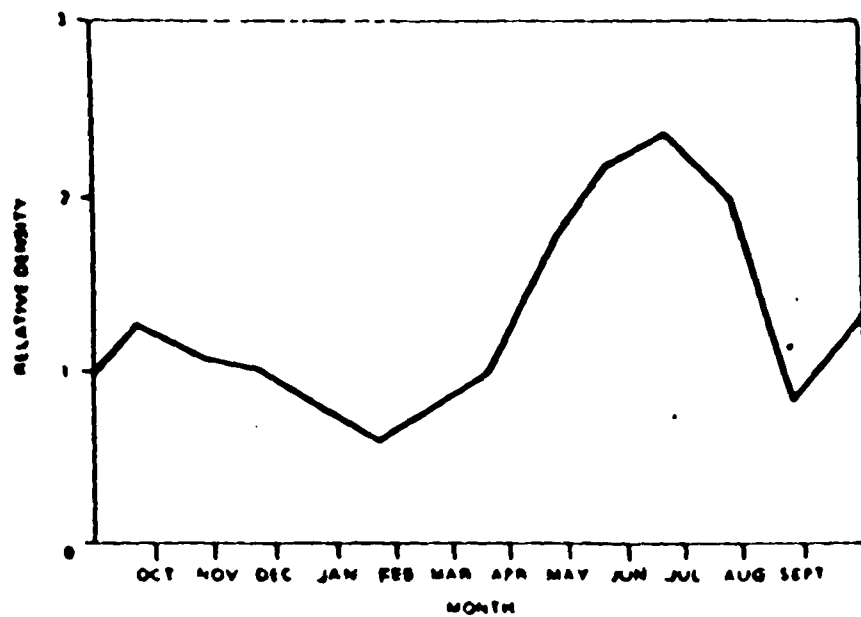
Table 1 — Order-of-Magnitude Estimates of the Properties of Sporadic Meteors [1]

Meteor Particles	Mass (g)	Radius	Number of This Mass or Greater Swept Up by the Earth Each Day	Electron Line Density (electrons per meter of trail length)
Particles pass through the atmosphere and fall to the ground	$10^4$	8 cm	10	—
Particles totally disintegrated in the upper atmosphere	$10^3$ $10^2$ 10 1	4 cm 2 cm 0.8 cm 0.4 cm	$10^2$ $10^3$ $10^4$ $10^5$	— — $10^{18}$ $10^{17}$
Approximate limit of radar measurements	$10^{-1}$ $10^{-2}$ $10^{-3}$ $10^{-4}$ $10^{-5}$ $10^{-6}$ $10^{-7}$ $10^{-8}$	0.2 cm 0.08 cm 0.04 cm 0.02 cm 80 $\mu\text{m}$ 40 $\mu\text{m}$ 20 $\mu\text{m}$ 8 $\mu\text{m}$	$10^6$ $10^7$ $10^8$ $10^9$ $10^{10}$ $10^{11}$ $10^{12}$ ?	$10^{16}$ $10^{15}$ $10^{14}$ $10^{13}$ $10^{12}$ $10^{11}$ $10^{10}$ ?
Micrometeorities (Particles float down unchanged by atmospheric collisions)	$10^{-9}$ $10^{-10}$ $10^{-11}$ $10^{-12}$	4 $\mu\text{m}$ 2 $\mu\text{m}$ 0.8 $\mu\text{m}$ 0.4 $\mu\text{m}$	Total for this group estimated as high as $10^{20}$	Practically none
Particles removed from the solar system by radiation pressure	$10^{-13}$ —	0.2 $\mu\text{m}$ —	— —	— —

Table 2  
AVERAGE INTERVAL BETWEEN DURSTS FOR THE  
COMET SYSTEM

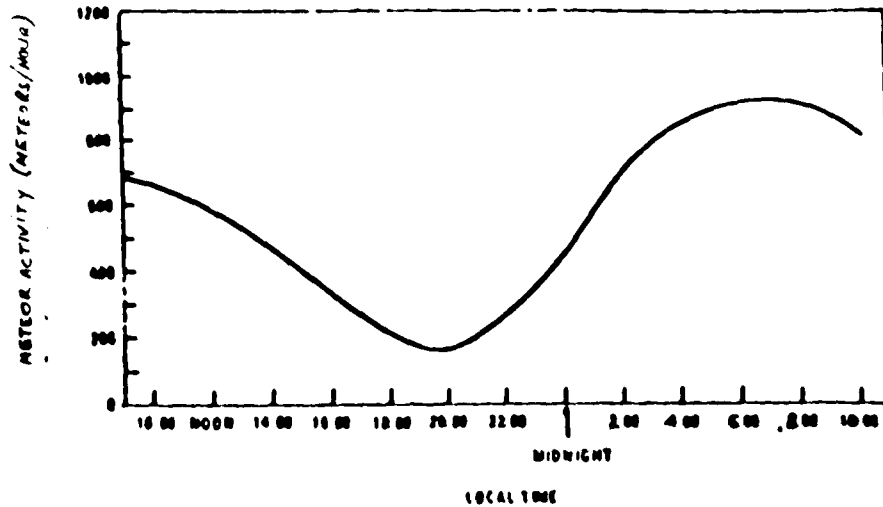
TIME OF DAY	JULY MAX	FEBRUARY min	YEARLY AVERAGE
4 AM MAX ACTIVITY	2.5 s	6.25 s	4 s
6 PM min ACTIVITY	25 s	16.67 s	20 s

## 7 FIGURES

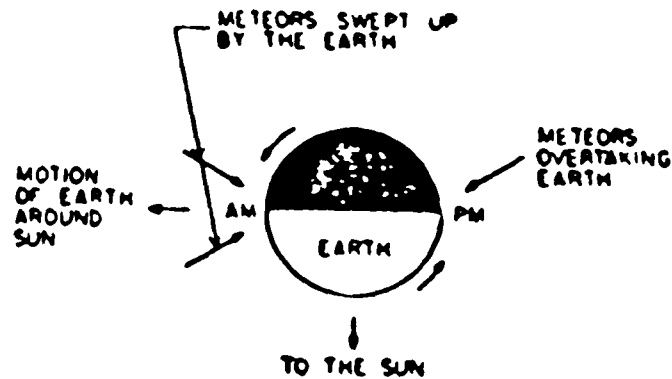


Variation in the space density of meteors along the Earth's orbit (reproduced from *Monthly Notices of the Royal Astronomical Society*, vol 116, by permission of The Royal Astronomical Society and G. S. Hawkins).

FIGURE 1

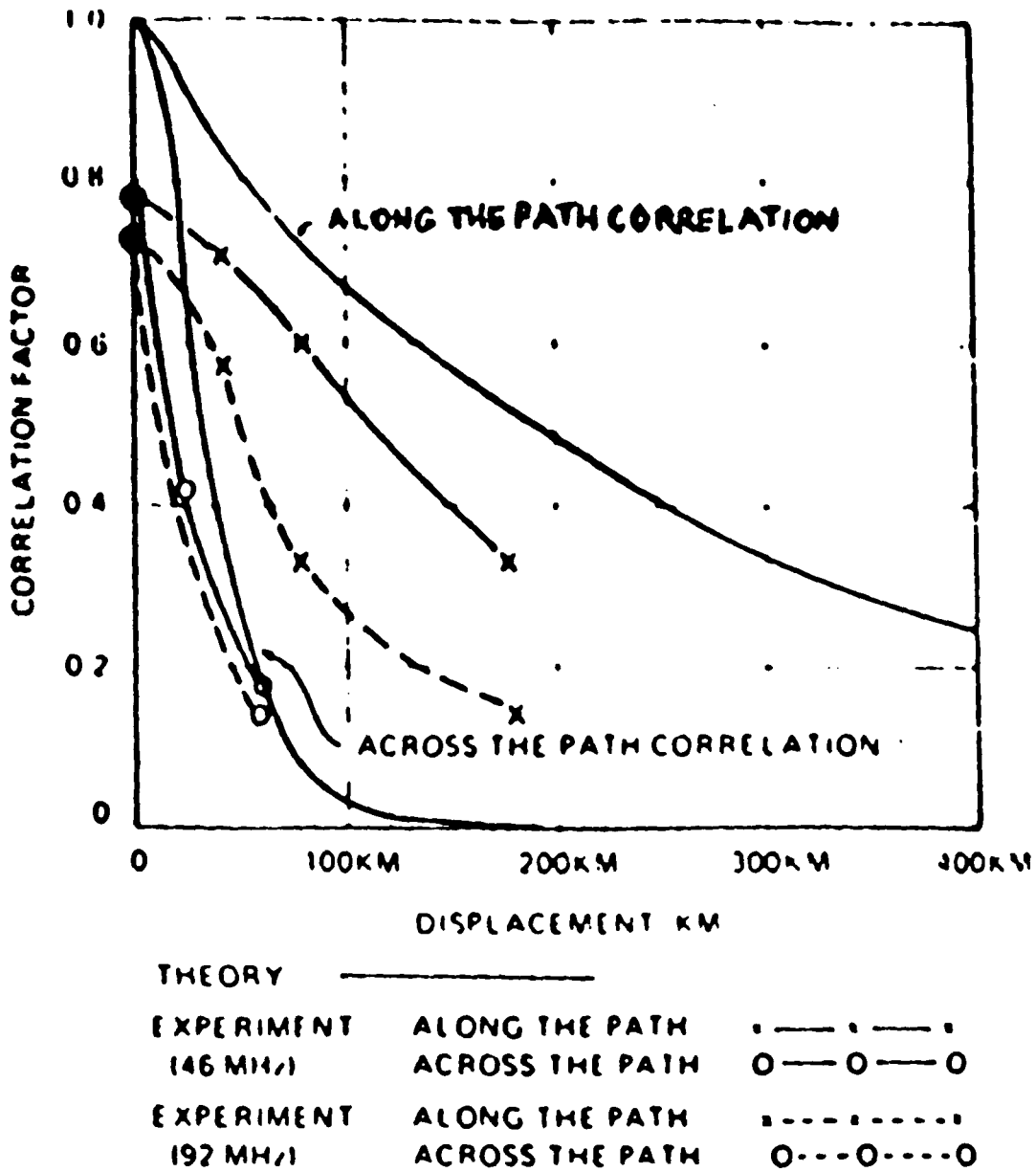


Diurnal variations in meteor activity.



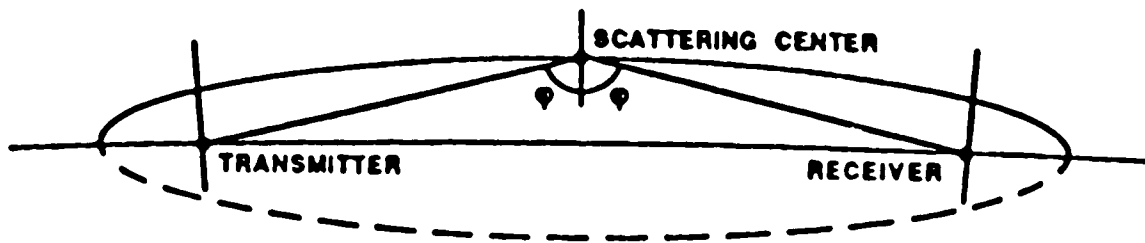
— Diurnal variations of meteor rates. In the evening only meteors overtaking the earth are observed. In the morning meteors with orbital directions opposite to that of the earth and the slower ones with the same orbital direction are observed.

FIGURE 2

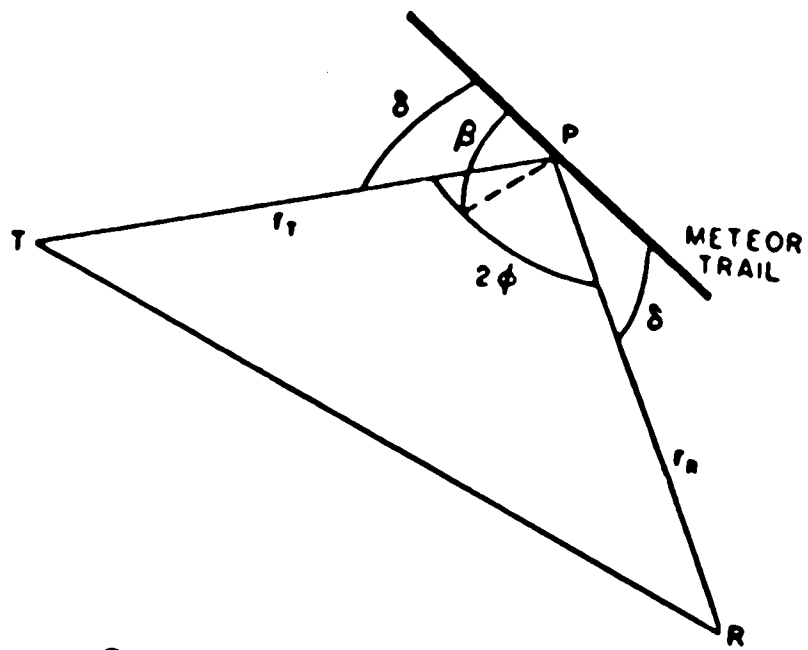


Correlation patterns in the vicinity of a meteor burst receiver

FIGURE 3

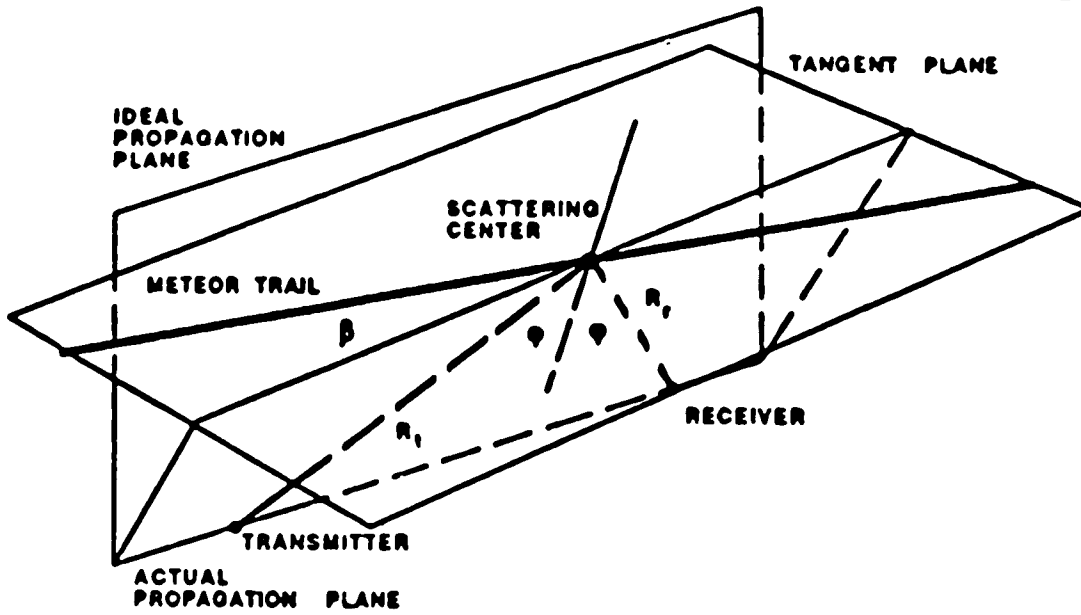


Link Geometry In the Ideal Propagation Plane

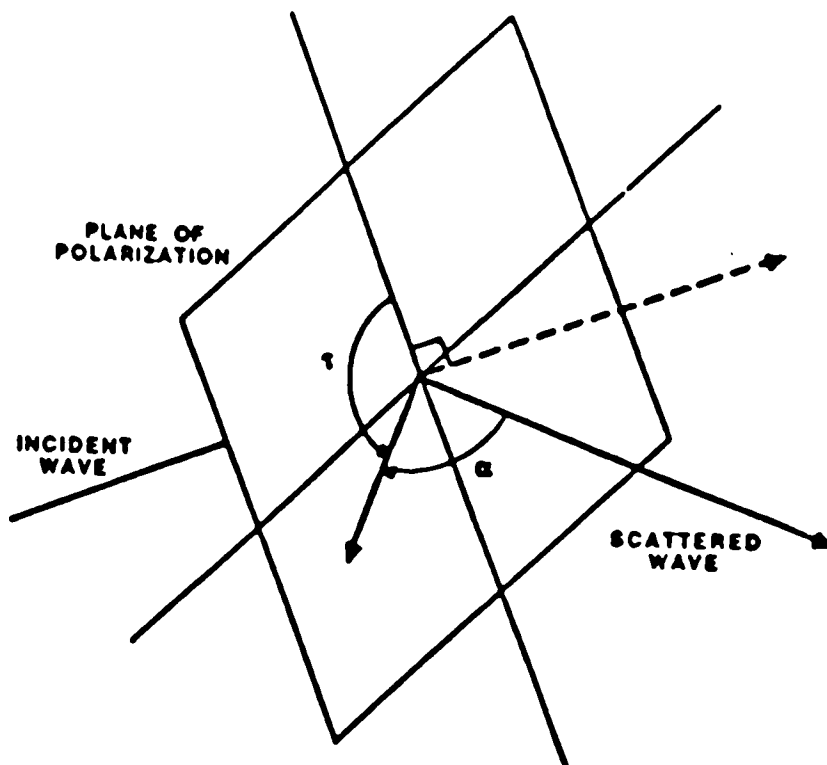


—Geometry of forward scattering from meteor trails.

FIGURE 4

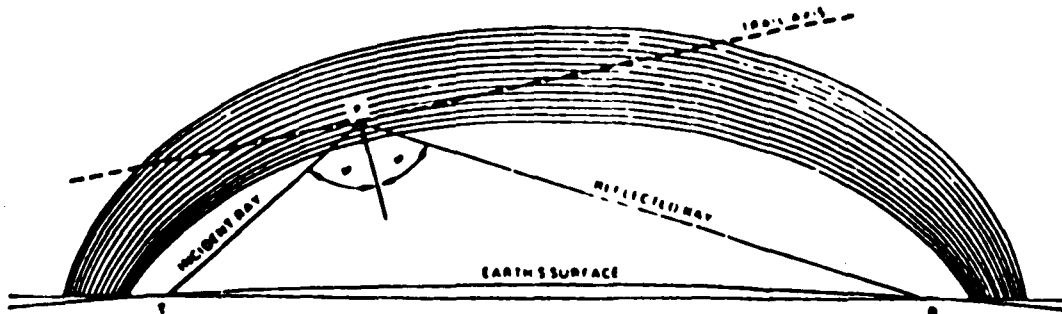


Meteor Scatter Communications Link Geometry



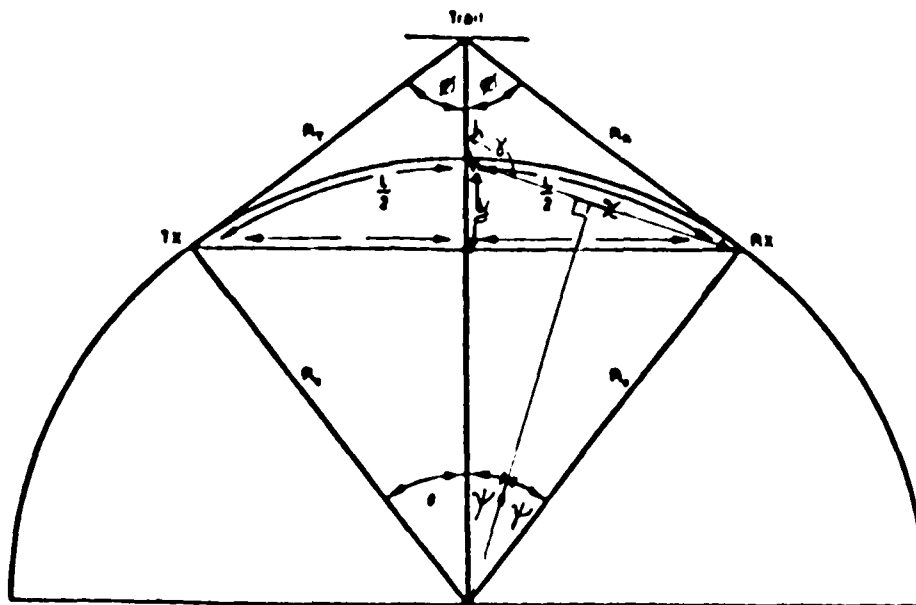
Polarization Geometry At Scattering Center

FIGURE 5



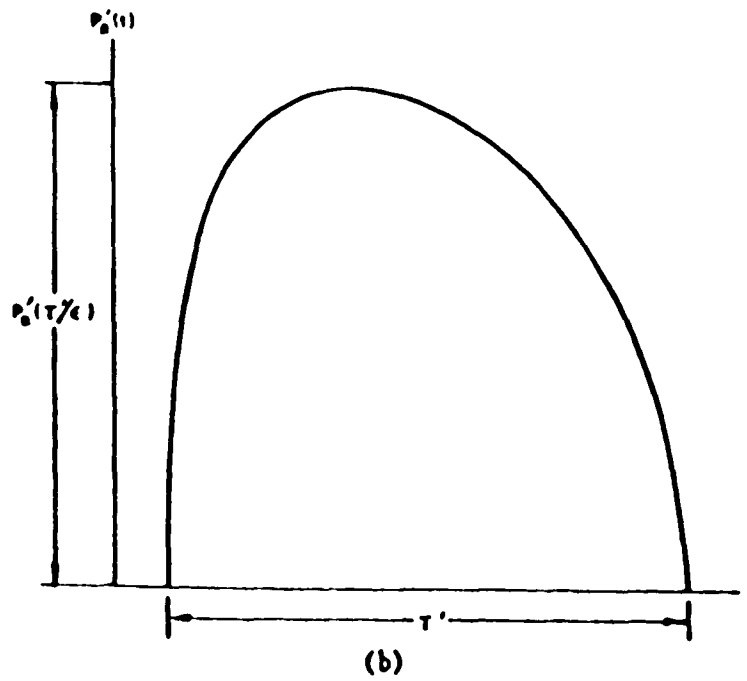
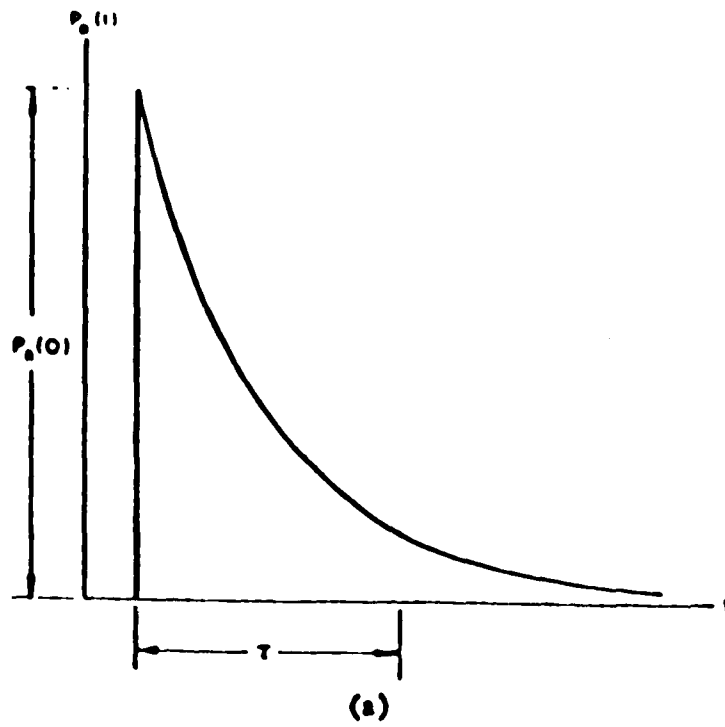
NOTE: ROTATION OF THE ELLIPSES GENERATES A FAMILY OF CONFOCAL PROLATE SPHEROIDS

Geometry of specular scattering from a meteor trail (reproduced from "The fine structure of meteor-burst signals" Tech. Memo. TM-36, Apr. 1962, by permission of the SRIAPL Technical Centre).



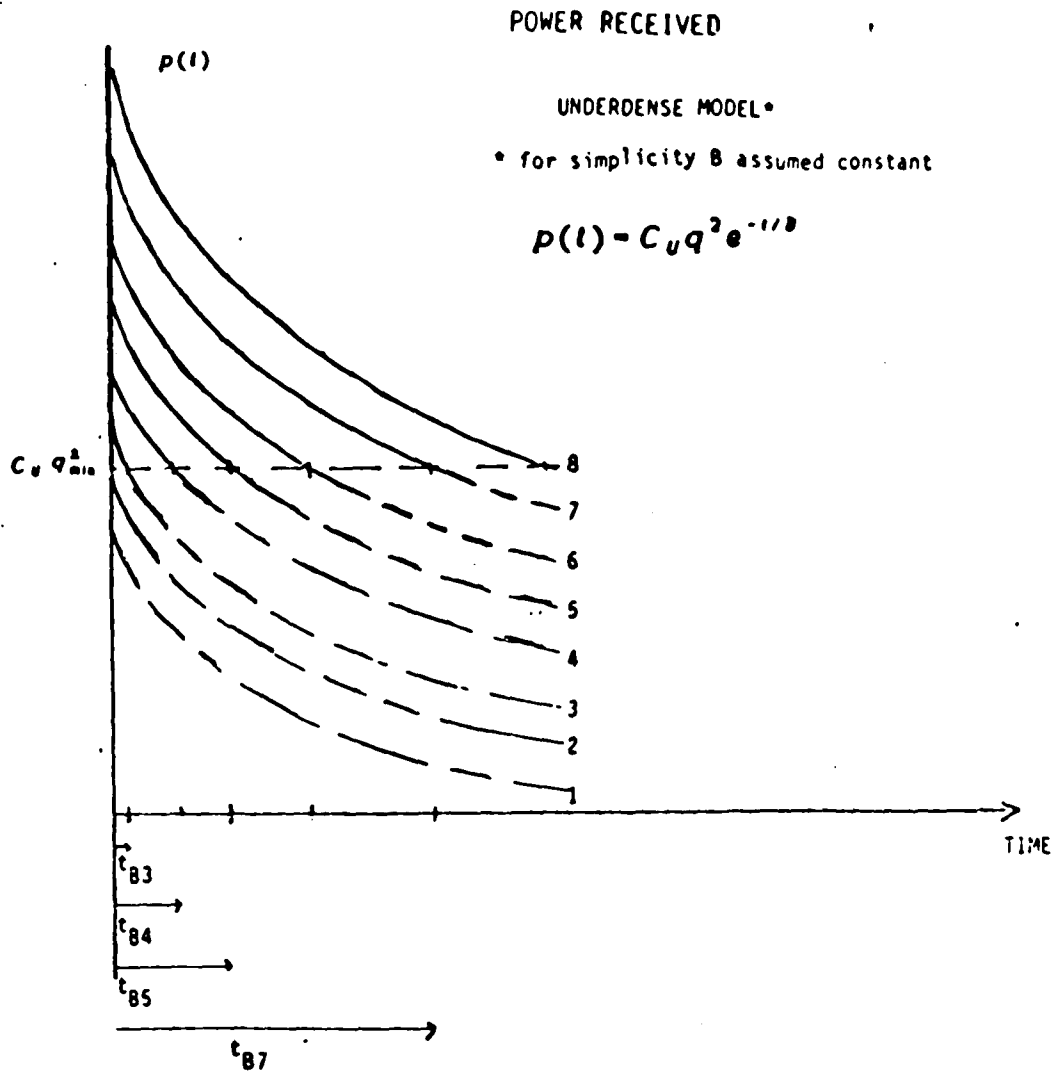
Meteor burst geometry. A signal from TX is reflected to RX by a trail that is  $h$  km above the earth. TX and RX are separated by a great circle distance of  $L$  km.

FIGURE 6



—Idealized time variations in signals from (a) underdense and (b) overdense meteor trails.

FIGURE 7



$C_U$ : Incorporates effects of transmitter power, antenna gains, link geometry, noise, ...

$q$ : Electron line density (random)  $q_L < q < q_U$

$B$ : Decay time constant (random)

$t_B$ : Channel "duration" ( $P > P_{min}$  for  $t < t_B$ )

--- no transmission

$P_{min}$ : Arbitrary, corresponds to max allowed BER, e.g. 10 dB

FIGURE 8

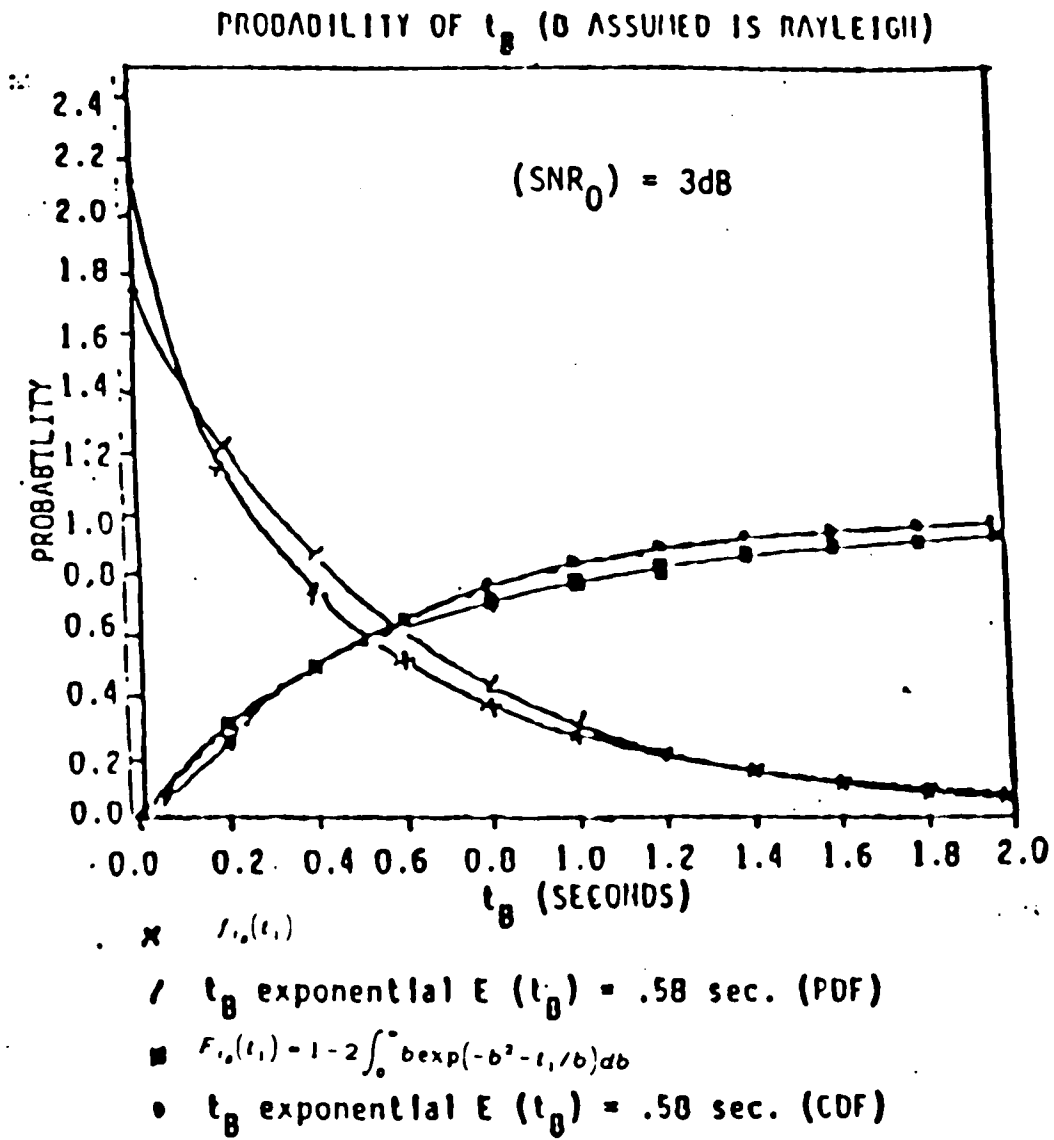
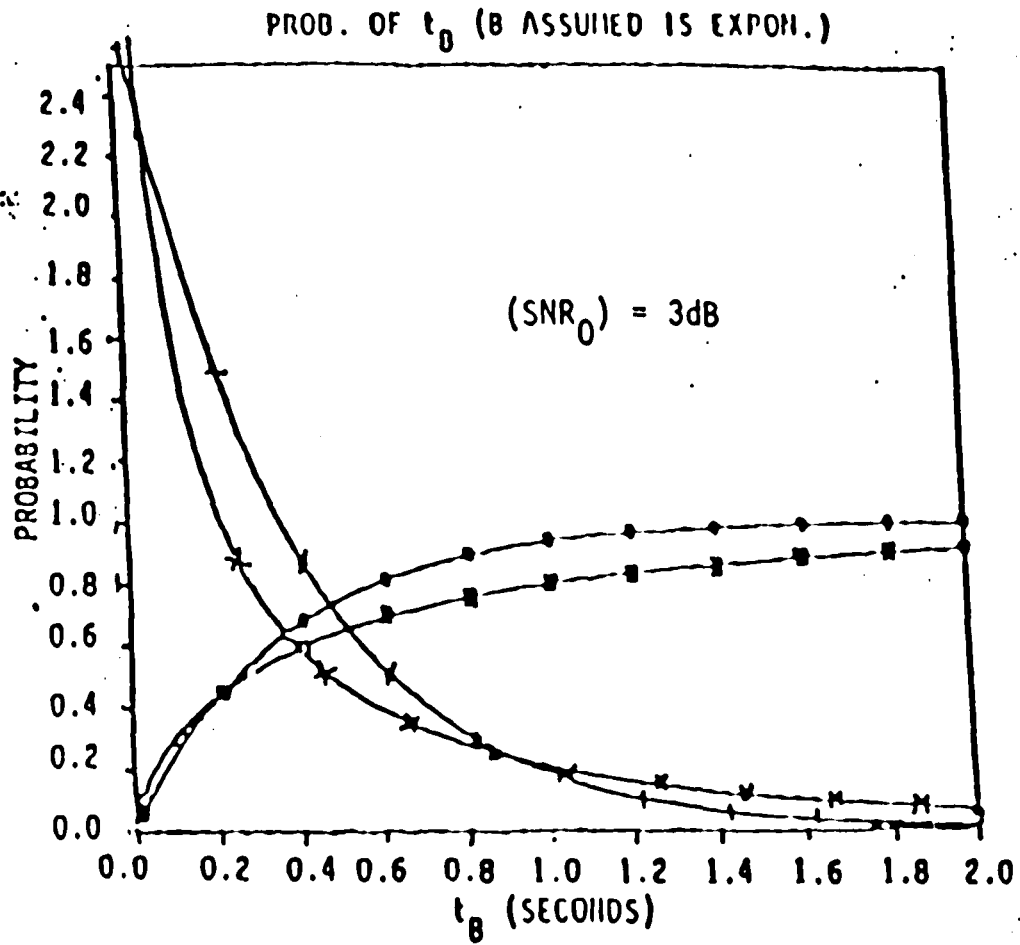


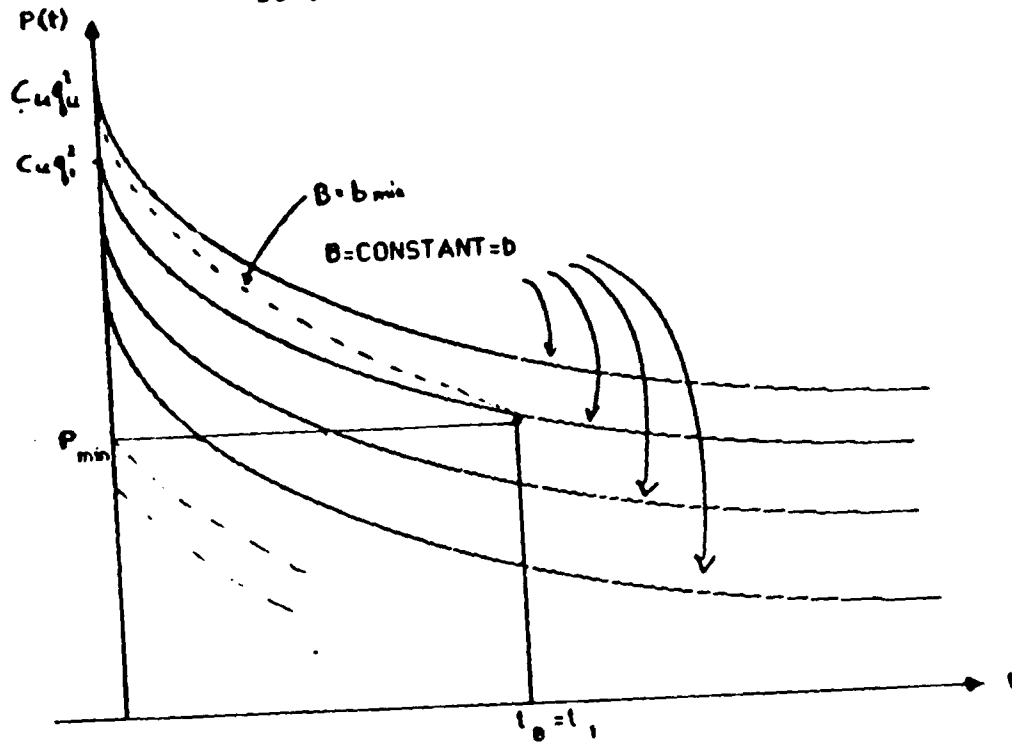
FIGURE 9



- x  $f_{t_0}(t_1) = 2 \frac{P_1}{B} K_0(z)$
- i  $t_B$  exponential  $E(t_0) = 0.377$  sec. (PDF)
- $F_{t_0}(t_1) = 1 - z K_1(z)$  where  $z = \sqrt{4 \frac{P_1}{B} t_1}$
- o  $t_B$  exponential  $E(t_0) = 0.377$  sec. (CDF)

FIGURE 10

BURST DURATION-UNDERDENSE



$$P_{min} = R \cdot N_0 \cdot g^{-1}(P_{b_{max}}) \quad q_v = q_{min} \cdot e^{t_1/2b}$$

$$Prob\{t_B \leq t_1 \mid B=b\} = \begin{cases} 0 & b \leq b_{min} \\ Prob\{q \leq q_v\} & b > b_{min} \end{cases}$$

$$t_0 = B \cdot \ln\left(\frac{q}{q_{min}}\right)^2$$

$$q_{min} = \sqrt{\frac{P_{min}}{C_u}}$$

$$P_{min} = N_0 \cdot R \cdot g^{-1}(P_{b_{max}})$$

FIGURE 11

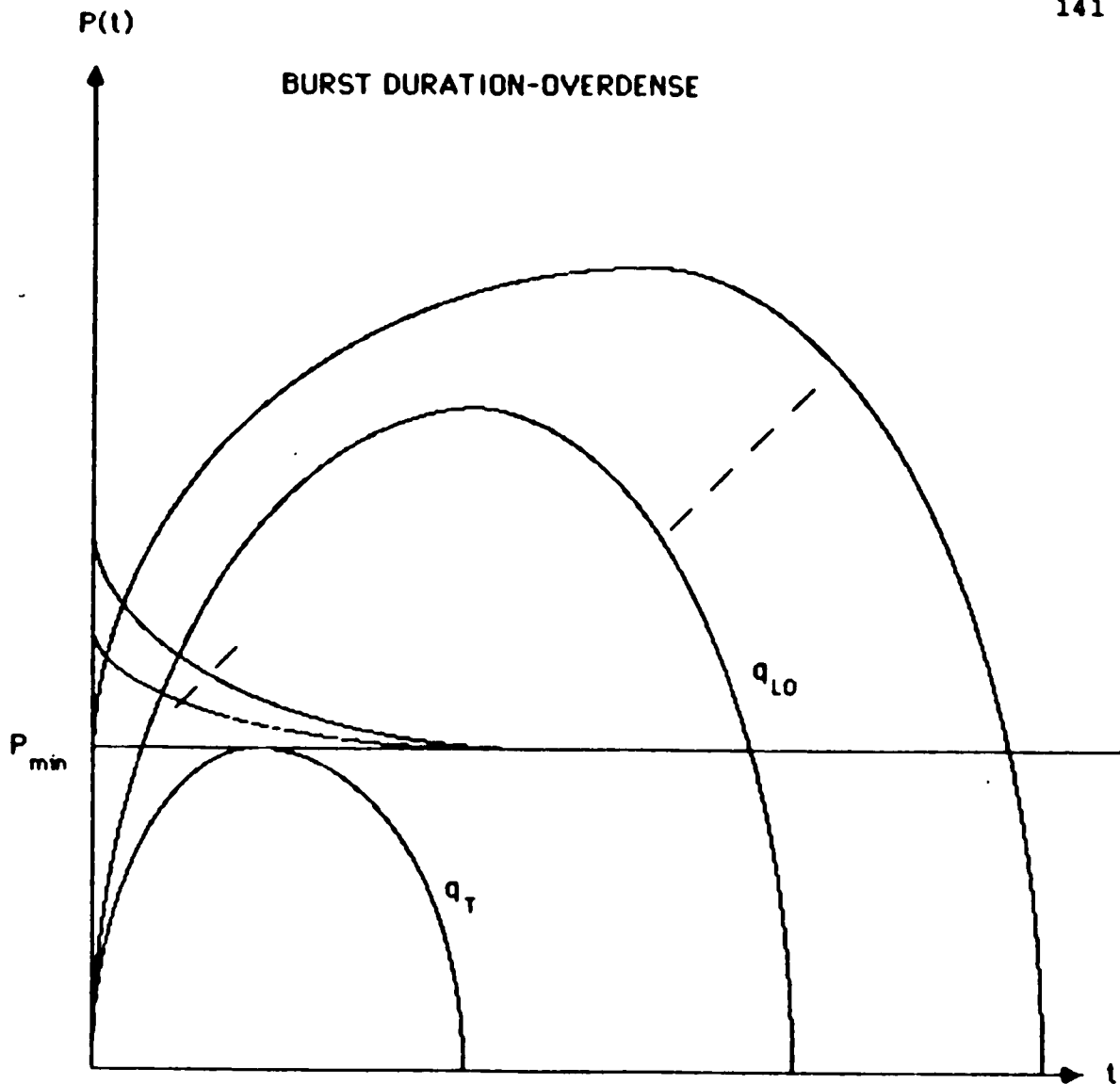


FIGURE 12

## BITS PER GIVEN BURST

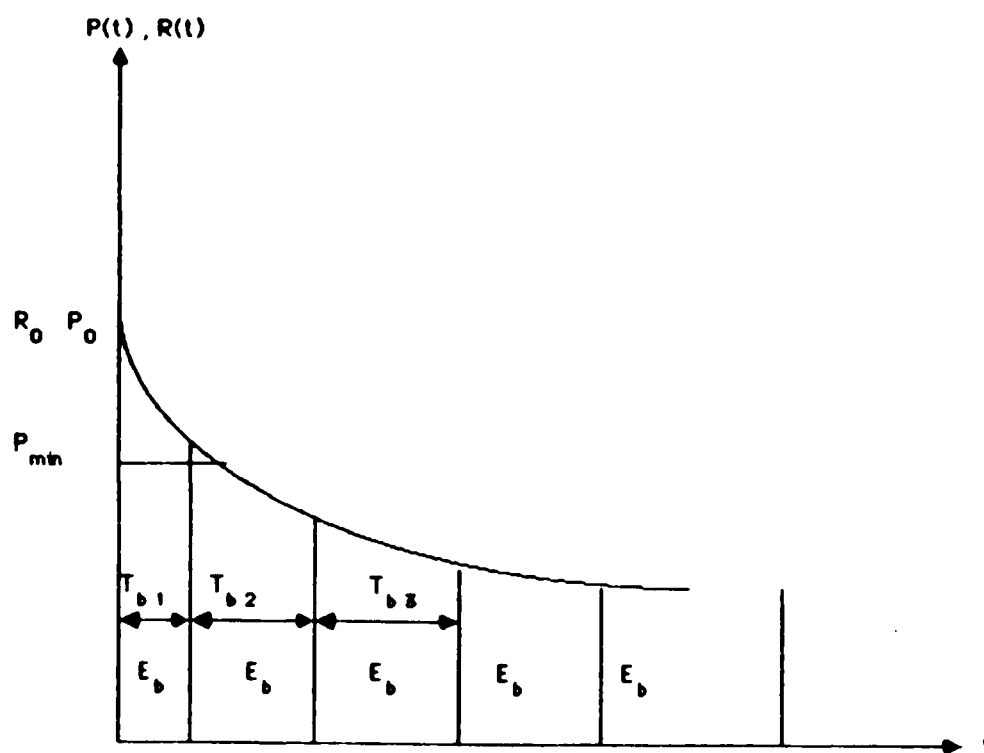
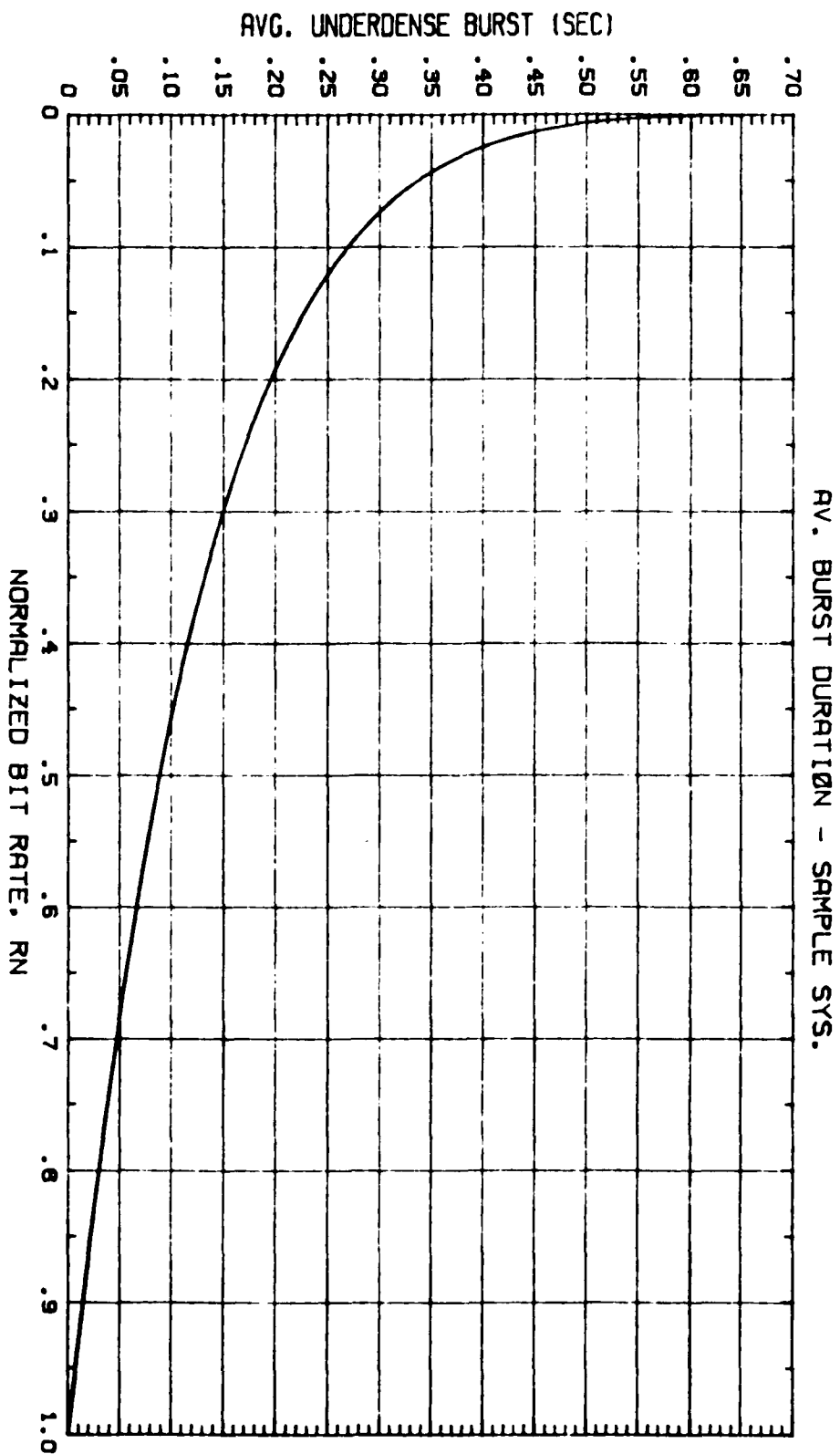
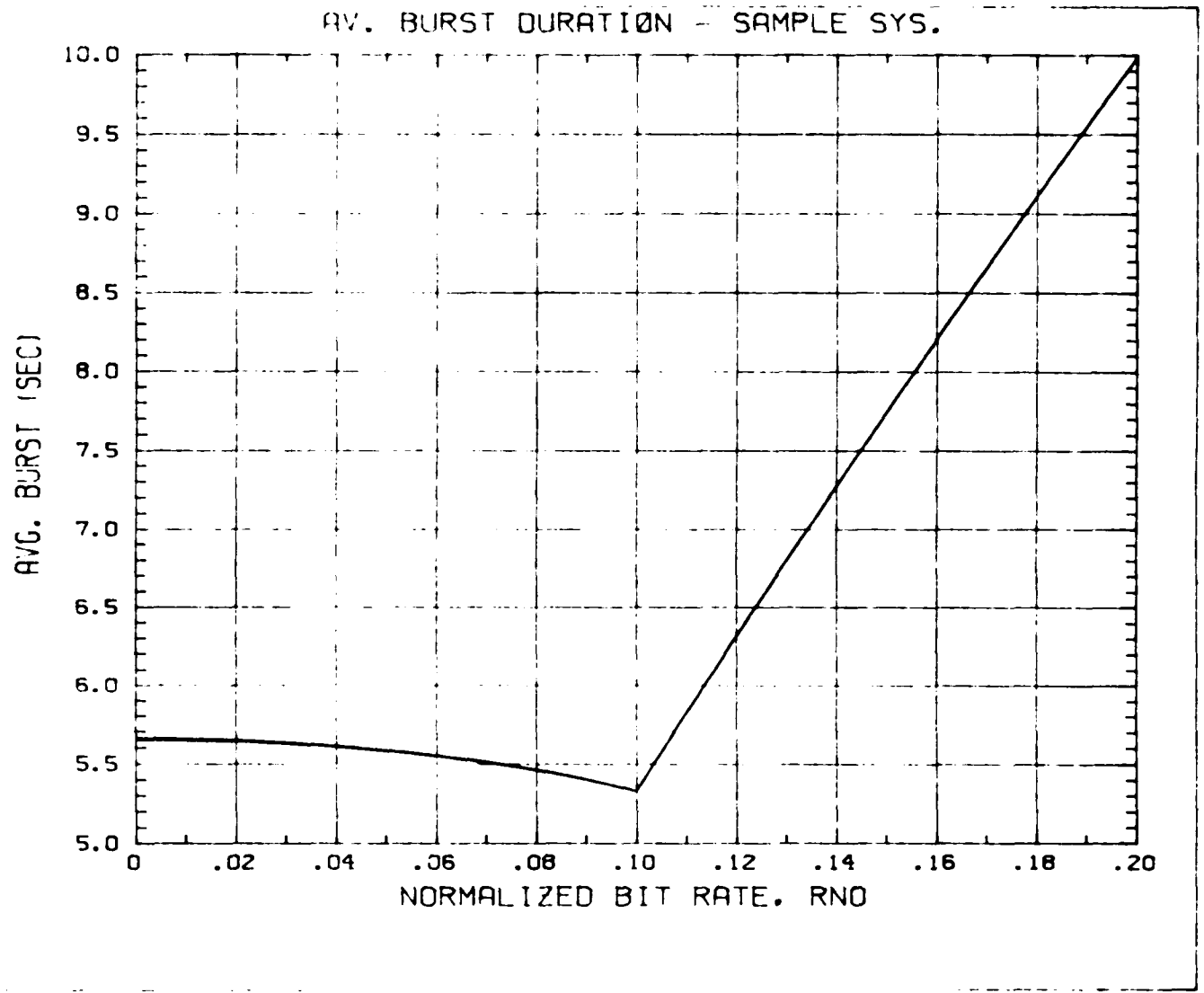
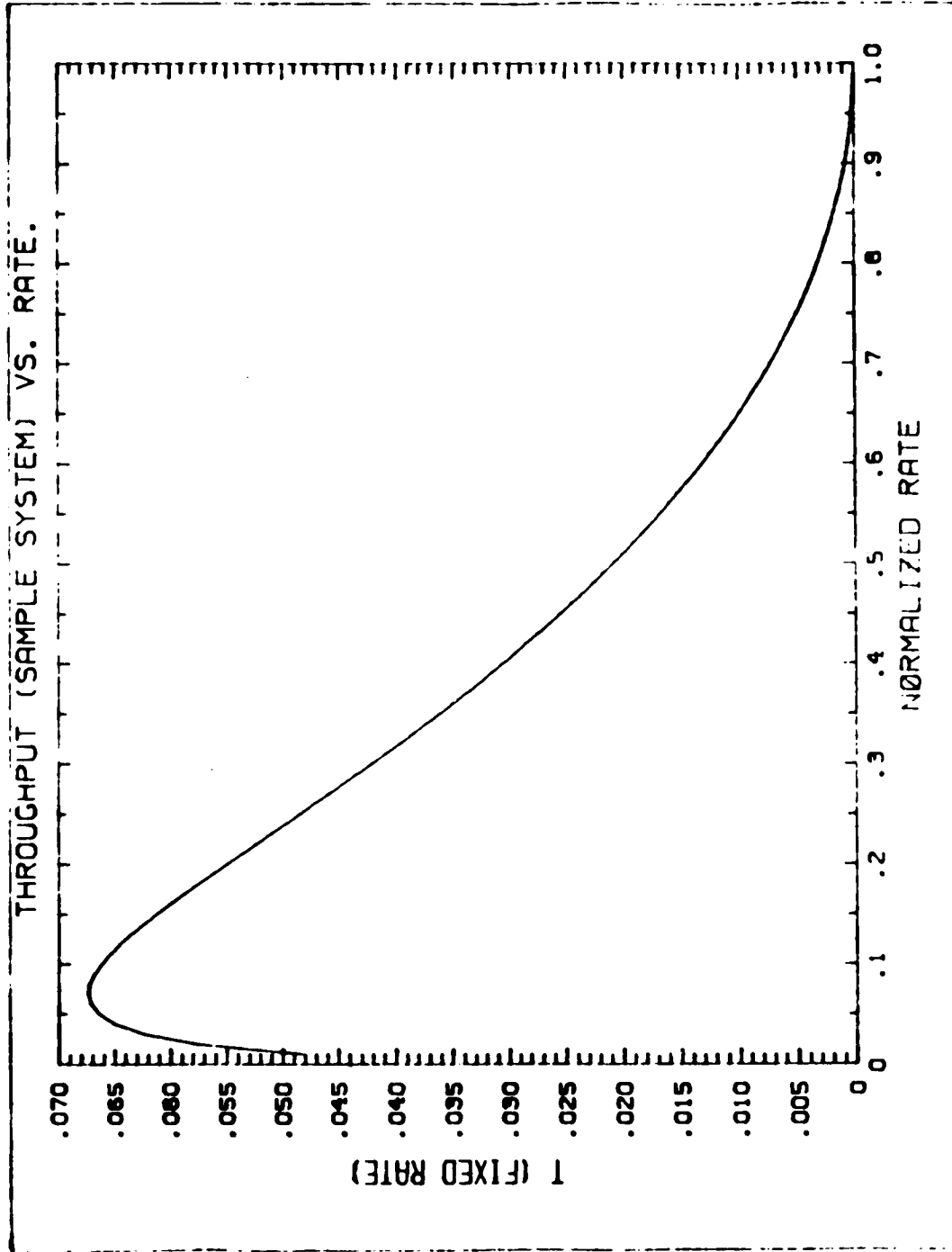


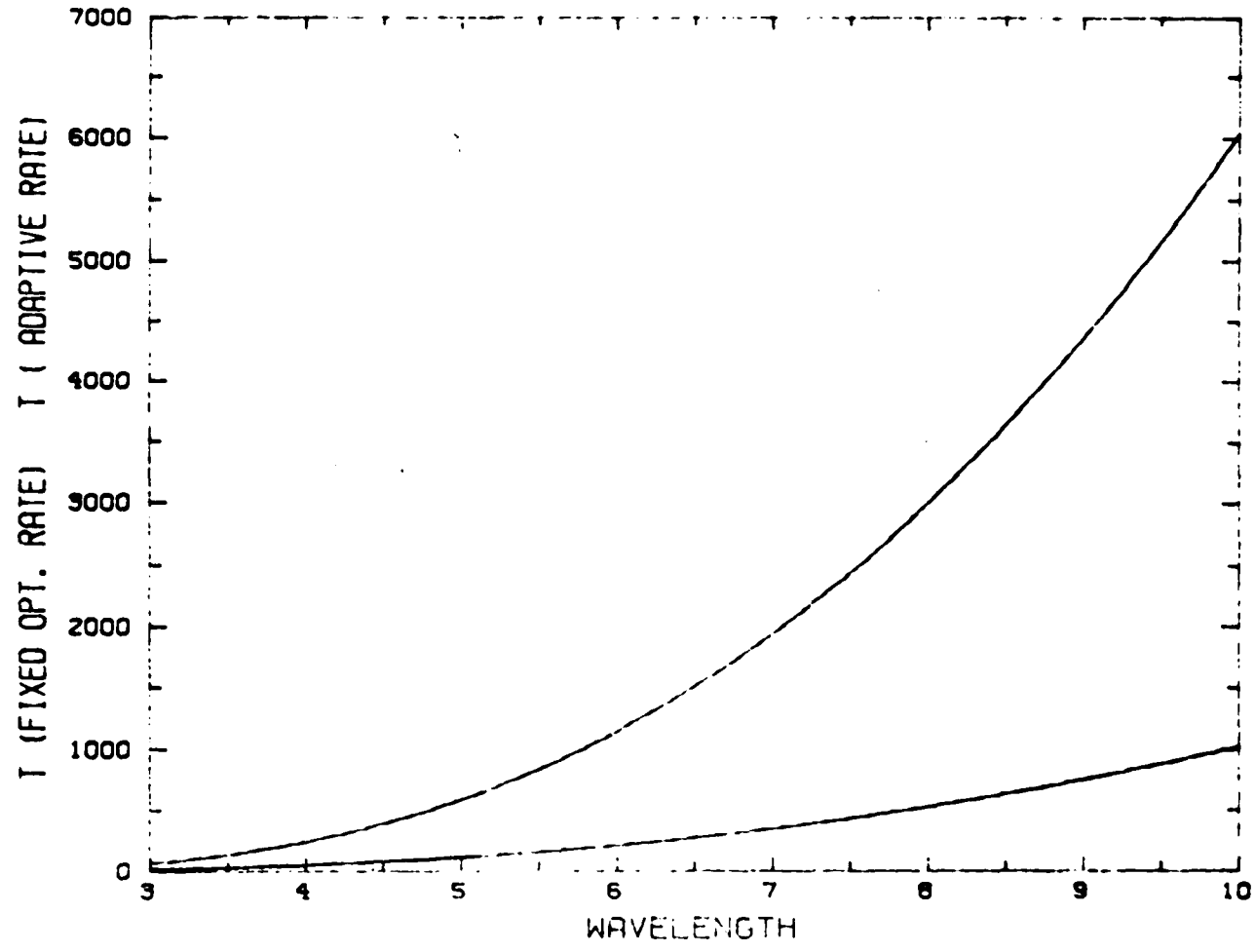
FIGURE 13



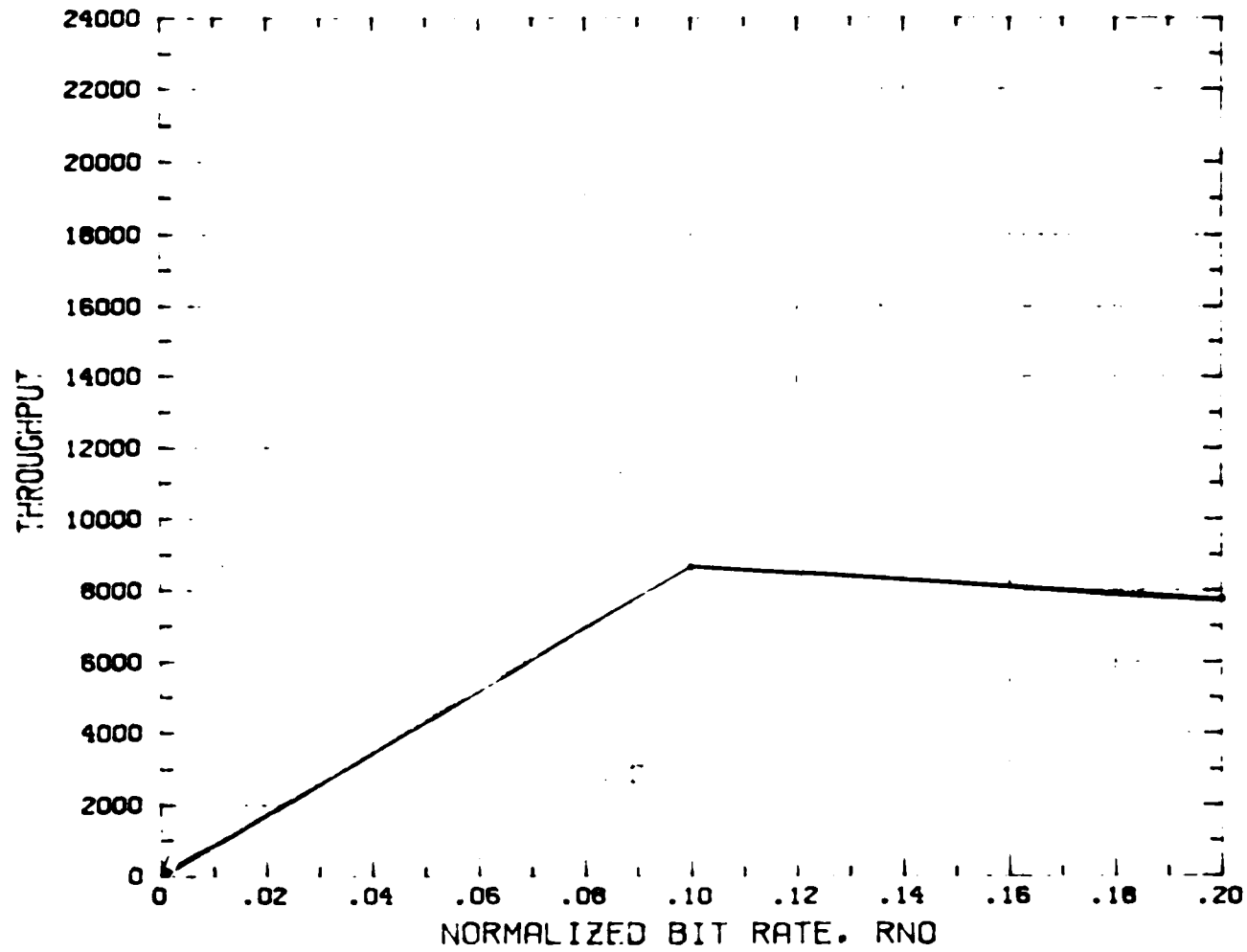




THROUGHPUT (SAMPLE SYSTEM) VS. WAVELEN.



THROUGHPUT - SAMPLE SYS.



## 8 REFERENCES

- [1] G.R. Sugar, "Radio propagation by reflection from meteor trails," Proc. IEEE, vol. 52, pp 116-136, Feb. 1964.
- [2] V.R. Eshleman and R.F. Mlodnosky, "Directional characteristics of meteor propagation derived from radar measurements," Proc. IRE, Dec. 1957.
- [3] P.J. Bartholome, "Results of propagation and interception experiments on the STC meteor-burst link", "SHAPE Tech. Cen. The Hague, The Netherlands, TM- 173, Dec. 1967.
- [4] P.A. Forsyth, E.L. Vogan, D.R. Hansen, and C.O. Hines, "The principles of JANET--A meteor-burst communications system," Proc. IRE, Dec. 1957.
- [5] P.J. Bartholome and I.M. Vogt, "Comet--A meteor-burst system incorporating ARQ and diversity reception," IEEE Trans. Commun. Technol., vol. COM-16, April 1968.
- [6] V.R. Eshleman and L.A. Manning "Radio Communications by Scattering from Meteoric Ionization", Proc IRE, Vol. 42, pp 530-536, March 1954.
- [7] A.E. Spezio, "Meteor burst communication system: Analysis and synthesis." NRL Rep. 8286, Dec. 28, 1978.
- [8] L.B. Milstein, D.L. Schilling, R.L. Pickholtz, J. Sellman, S. Davidovici, A. Pavelchek, A. Schneider, G. Eichmann, "Performance of Meteor Burst Communication Channels", to be published.
- [9] J.D. Oetting, "An analysis of meteor burst communications for military applications," IEEE Trans. Commun., vol. COM-28, pp. 1591-1601, Sept. 1980
- [10] J.A. Weitzen, W.P. Biro kenmeier, and M.D. Grossi, "An estimate of the capacity of the meteor burst channel," IEEE Trans. Commun., vol. COM-32, pp. 972-974, Aug. 1984.
- [11] M.W. Abel, Meteor Burst Communications: Bits per Burst Performance Bounds" IEEE Trans. Commun., vol. COM-34, pp.927-936, Sep. 1986.
- [12] Hibshoosh, E., Schilling, D.L., Time Varying Bit Error Rate for Meteor Burst Channel, MILCOM'86, Monterey, CA, Oct. '86.

[13] Osterjaard, J.C., Ramusen, J.E., Sousa, M.J., Quinn, M.J. and Kossey, P.A., Characteristics of High Latitude Meteor Scatter Propagation Parameters Over the 45-104 MHz Band, RADC Publications.

[14] Report 631-2 (MOD F); Frequency Sharing Between the Broadcasting-Satellite Service (sound and television) and Terrestrial Services. Recommendations and Reports of the CCIR, 1982, Vol X/Xi-2.

[15] Report 540-1; (MOD F); The Use of Frequency Bands Allocating to the Fixed-Satellite Service for Both the Up Link and Down Link of Geostationary-Satellite Systems. Ibid, Vol IV-1.

[16] C.O. Hines and P.A. Forsyth, "The Forward Scattering of Radio Waves from Overdense Meteor Trails", Canad. J. Physics, Vol. 35, Feb. 1957.

[17] Withers, D.J., Durkin, J., Frequency Band Sharing and Warc-Orb-85, June 22-25, 1986, Presented at ICC'86, Toronto, Ontario, Canada.

[18] Bello, P.A., Some Techniques for the Instantaneous Real-Time Measurement of Multipath and Doppler Spread, Sept. 1965, IEEE Trans. on Comm. Tech.

[19] Bello, P.A., Error Probabilities Due to Atmospheric Noise and Flat Fading in HF Ionospheric Communication Systems, Sept. 1965, IEEE Trans. on Comm. Tech.

[20] Watterson, C.C., Juroshek, J.R., Bensema, W.D., Experimental Confirmation of an HF Channel Model, Dec. 1970, IEEE Trans. on Comm. Tech.

[21] J.Hampton, "A Meteor Burst Model With Time Varying Bit Error Rate", Milcom 1985, 32.2.1.

[22] SEMCOR, Inc., Regency Net Project, Meteor Burst Signalling Architecture study Final Report, Dec. 1985.

[23] Schanker, J.Z., Meteor Burst Communication Systems, September 5-9, 1983, IREECON International Sydney '83, 19th International Electronics Convention and Exhibition, Digest of Paper, pp 183-5. Sydney, Australia.

- [24] L.A. Manning and V.R. Eshleman, "Meteors in the ionosphere", Proc. IRE, vol 47, pp. 186-199, February 1959.
- [25] O.G. Villard, et al., "The role of meteors in extended range VHF propagation, Proc. IRE, vol 43, pp 1473-1481, October 1955.
- [26] G.S. Hawkins, "A radio survey of sporadic meteor radiants," Monthly Notices Roy., Astron. Soc, vol. 116, pp 92-104, November 1956.
- [27] G.S. Hawkins, "Variation in the occurrence rate of meteors", Astron, J. vol 61, pp 386-391, Nov. 1956.
- [28] Western Union Gov. Syst Div. "Western Union meteor burst communications systems overview", Inform Brochure, Jan 1977.
- [29] V.R. Eshelman, L.A. Manning, A.M. Peterson and O.G. Villard, Jr. "Some Properties of oblique radio reflections from meteor ionization trails", J. Geophys Res., vol 61, pp 233-249, June 1956.
- [30] C.O. Hines and R.E. Pugh, "The spatial distribution of signal sources in meteoric forward scattering", Canad. J. Phys, vol. 34, pp 1005-1015, Oct. 1956.
- [31] O.G. Villard, et al, "Some properties of oblique radio reflections from meteor ionization trails", J. Graphys. Res., vol 61, pp 233-249, June 1956.
- [32] J.A. Weitzen, M.D. Grossi and W.P. Birkemeier, "High resolutions multipath measurements of the meteor scatter channel," Radio Sci. Jan. 1984.
- [33] J.A, Weitzen, Signetron Corp., Private Communications.
- [34] IBM Corp., MBC Model Communication Assessment Program, (rev. 3.0).
- [35] Abramowitz and Stegun, "Handbook of Mathematical Functions", Dover Pub, pp. 1001-1003.